

Disintegration of beauty: a precision study

Alexander Lenz,^a Maria Laura Piscopo,^a Aleksey V. Rusov^a

^a*Physik Department, Universität Siegen, Walter-Flex-Str. 3, 57068 Siegen, Germany*

E-mail: alexander.lenz@uni-siegen.de, maria.piscopo@uni-siegen.de,
rusov@physik.uni-siegen.de

ABSTRACT: We update the Standard Model (SM) predictions for B -meson lifetimes within the heavy quark expansion (HQE). Including for the first time the contribution of the Darwin operator, $SU(3)_F$ breaking corrections to the matrix element of dimension-six four-quark operators and the so-called eye-contractions, we obtain for the total widths $\Gamma(B^+) = (0.58_{-0.07}^{+0.11}) \text{ ps}^{-1}$, $\Gamma(B_d) = (0.63_{-0.07}^{+0.11}) \text{ ps}^{-1}$, $\Gamma(B_s) = (0.63_{-0.07}^{+0.11}) \text{ ps}^{-1}$, and for the lifetime ratios $\tau(B^+)/\tau(B_d) = 1.086 \pm 0.022$, $\tau(B_s)/\tau(B_d) = 1.003 \pm 0.006 (1.028 \pm 0.011)$. The two values for the last observable arise from using two different sets of input for the non-perturbative parameters $\mu_\pi^2(B_d)$, $\mu_G^2(B_d)$, and $\rho_D^3(B_d)$ as well as from different estimates of the $SU(3)_F$ breaking in these parameters. Our results are overall in very good agreement with the corresponding experimental data, however, there seems to emerge a tension in $\tau(B_s)/\tau(B_d)$ when considering the second set of input parameters. Specifically, this observable is extremely sensitive to the size of the parameter $\rho_D^3(B_d)$ and of the $SU(3)_F$ breaking effects in μ_π^2 , μ_G^2 and ρ_D^3 ; hence, it is of utmost importance to be able to better constrain all these parameters. In this respect, an extraction of $\mu_\pi^2(B_s)$, $\mu_G^2(B_s)$, $\rho_D^3(B_s)$ from future experimental data on inclusive semileptonic B_s -meson decays or from direct non-perturbative calculations, as well as more insights about the value of $\rho_D^3(B)$ extracted from fit, would be very helpful in reducing the corresponding theory uncertainties.

Contents

1	Introduction	1
2	Theoretical framework	5
2.1	Effective Hamiltonian and HQE	5
2.2	Short-distance contributions	8
2.3	Non-perturbative input	11
3	Numerical analysis and results	16
4	Conclusion	20
A	Numerical input	23
B	Dimension-seven four-quark operator contribution in VIA	25

1 Introduction

The total decay width Γ or equivalently its inverse, the total lifetime $\tau = \Gamma^{-1}$, defines one of the fundamental properties of elementary and composite particles, and hence represents an observable of phenomenological primary importance. Moreover, in particular for the case of heavy hadrons, the study of lifetimes can provide an interesting playground to test our understanding of the weak and the strong interactions.

Experimentally, the lifetimes of B mesons are determined very precisely by now [1] (based on the measurements in Refs. [2–61]). The values in Table 1 show that the lightest B mesons

	B^+	B_d	B_s
τ [ps]	1.638 ± 0.004	1.519 ± 0.004	1.516 ± 0.006
Γ [ps^{-1}]	0.6105 ± 0.0015	0.6583 ± 0.0017	0.6596 ± 0.0026
$\tau(B_q)/\tau(B_d)$	1.076 ± 0.004	1	0.998 ± 0.005

Table 1: Status of the experimental determinations of the B -meson lifetimes [1].

have roughly the same lifetime and that in the ratio $\tau(B_s)/\tau(B_d)$ all differences seem to almost cancel out. The improvement of the experimental determination for this ratio over the last

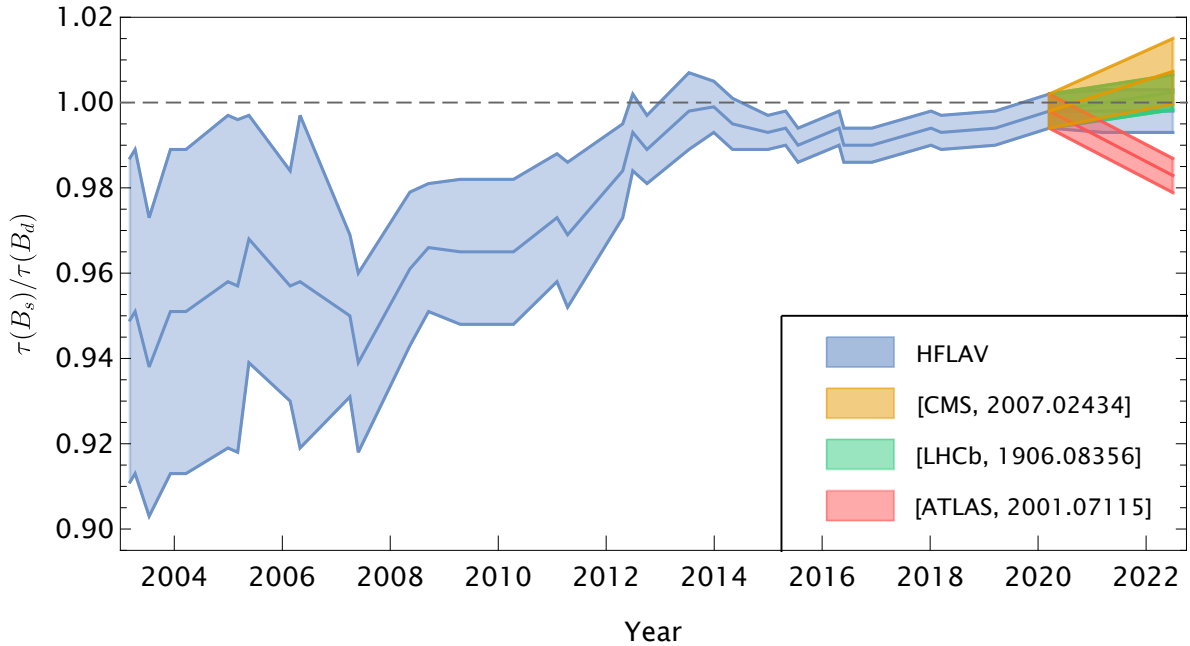


Figure 1: HFAG/HFLAV results for the lifetime ratio $\tau(B_s)/\tau(B_d)$ from 2003 till 2022. Note, that the recent measurements of Γ_s by ATLAS (red) seem to deviate from the most recent determinations by LHCb (green) and CMS (orange); the corresponding bands are in fact obtained by fixing the current HFLAV value for $\tau(B_d)$.

20 years can be read off Fig. 1. Interestingly, the recent measurement of Γ_s by ATLAS [56] deviates from the most recent ones by LHCb [62–64] and CMS [58] by $2-4\sigma$ - an experimental clarification of the origin of these discrepancies is of course highly desirable.

On the theoretical side, inclusive decay widths of heavy hadrons can be systematically computed in the framework of the heavy quark expansion (HQE), see e.g. the review [65]. Predictions for lifetime ratios of B mesons based on this method trace back to the 80s and a selection of results is given in Table 2. According to the HQE the total decay rate of the B_q

	$\tau(B^+)/\tau(B_d)$	$\tau(B_s)/\tau(B_d)$
Shifman, Voloshin, 1986 [66]	≈ 1.1	≈ 1
Neubert, Sachrajda, 1996 [67]	fixed to 1.02	$1 \pm \mathcal{O}(1\%)$
Gabbiani et al., 2004 [68]	1.06 ± 0.02	1.00 ± 0.01
Kirk et al., 2017 [69]	$1.082^{+0.022}_{-0.026}$	1.0007 ± 0.0025

Table 2: Selected theoretical determinations of the B -meson lifetimes.

meson, $\Gamma(B_q)$, with $q = (u, d, s)$ ¹, can be expressed as a series expansion in inverse powers of the heavy quark mass. Due to the large value of the b -quark mass in comparison to a typical hadronic scale, we expect a good convergence of the HQE for B mesons. Moreover, recent studies of D meson lifetimes [73, 74] and charmed baryon lifetimes [74] indicate a convergence of the HQE even in the charm system.

In the framework of the HQE, $\Gamma(B_q)$ can be split up into the sum of a leading contribution stemming from the decay of the free heavy b -quark, Γ_b , and of a subleading one which is specific to the B_q meson, $\delta\Gamma_{B_q}$:

$$\Gamma(B_q) = \Gamma_b + \delta\Gamma_{B_q}. \quad (1.1)$$

We stress that the free quark decay is proportional to the factor $\Gamma_0 = G_F^2 m_b^5 |V_{cb}|^2 / (192\pi^3)$ and hence has a strong dependence on the mass of the decaying quark. Similarly, ratios of B -meson lifetimes can be recast, without making any approximations, as:

$$\frac{\tau(B_q)}{\tau(B_{q'})} = \frac{\Gamma_b + \delta\Gamma_{B_{q'}}}{\Gamma_b + \delta\Gamma_{B_q}} = 1 + \left(\delta\Gamma_{B_{q'}} - \delta\Gamma_{B_q} \right) \tau(B_q). \quad (1.2)$$

In our analysis we obtain predictions for the lifetime ratios by combining the HQE result for $(\delta\Gamma_{B_{q'}} - \delta\Gamma_{B_q})$ with the experimental value of $\tau(B_q)$, given the higher precision of the latter. Note that in this way, the numerically leading term Γ_b cancels out, so that $\tau(B_q)/\tau(B_{q'})$ becomes sensitive only to subleading HQE corrections, while the total decay rate can be used primarily to test our ability to predict the free-quark decay. Alternatively, Eq. (1.2) can be determined entirely within the HQE, in this case the dependence on Γ_b is still present albeit very mildly, leading to slightly larger uncertainties.

In the presence of physics beyond the SM (BSM), lifetime ratios will be modified as:

$$\begin{aligned} \frac{\tau(B_q)}{\tau(B_{q'})} &= 1 + \left(\delta\Gamma_{B_{q'}}^{\text{SM}} - \delta\Gamma_{B_q}^{\text{SM}} \right) \tau(B_q) \\ &+ \text{Br}(B_{q'} \rightarrow X)^{\text{BSM}} \frac{\tau(B_q)}{\tau(B_{q'})} - \text{Br}(B_q \rightarrow Y)^{\text{BSM}}. \end{aligned} \quad (1.3)$$

For the case of the ratio $\tau(B_s)/\tau(B_d)$, a precision of the per mille level - both in experiments and theory - will allow indirect new physics searches $B_q \rightarrow X$ at the same level of accuracy. However, also a precision of the order of one or two per cent in the theory prediction of $\tau(B^+)/\tau(B_d)$ can give interesting constraints on certain BSM models. Examples of new $B_q \rightarrow X$ transitions that can modify the predictions for the B -meson lifetimes are:

- BSM contributions to non-leptonic tree-level b -quark decays, like $b \rightarrow c\bar{u}d$, $b \rightarrow c\bar{u}s$ or $b \rightarrow c\bar{c}s$ transitions, see e.g. Refs. [75–82].
- BSM effects to $b \rightarrow s\tau\tau$ transitions, see e.g. Ref. [83] - such enhanced contributions could stem from models that explain the $b \rightarrow s\ell\ell$ anomalies, see e.g. Refs. [84–86]. Moreover,

¹Note that we only consider bound states of the b and a light quark. In the case of the B_c meson the HQE must be properly generalised to describe two weakly decaying heavy quarks, see Refs. [70–72].

direct bounds on this channel are very weak [87], and in the range of the experimental precision of the lifetime ratio $\tau(B_s)/\tau(B_d)$:

$$\text{Br}(B_s \rightarrow \tau^+\tau^-) < 6.8 \cdot 10^{-3} \quad (\text{LHCb}). \quad (1.4)$$

The corresponding SM prediction [88] lies far below the current experimental bound:

$$\text{Br}(B_s \rightarrow \tau^+\tau^-)^{\text{SM}} = (7.73 \pm 0.49) \cdot 10^{-7}. \quad (1.5)$$

- BSM contributions that arise in the baryogenesis models presented in Refs. [89, 90] contain new b -quark decay channels that affect the lifetimes.

We also point out that a precise determination of $\tau(B_s)/\tau(B_d)$ and $\tau(B^+)/\tau(B_d)$ can be further used to constrain the possible size of duality violating effects in the theoretical determination of lifetimes, see Ref. [91].

In light of the increasing experimental precision and of the phenomenological potential outlined above, we present an update of the SM prediction for B -meson lifetimes. Specifically, our study includes the following improvements with respect to previous works:

1. The Wilson coefficient of the Darwin operator. This represents a correction of order $1/m_b^3$ to the HQE and only recently the corresponding expressions for non-leptonic b -quark decays have been computed in Refs. [92–95]. Thus, in the present work we include for the first time the complete dimension-six contribution at LO-QCD. Interestingly, the Darwin operator leads to sizeable effects to the lifetimes and in particular constitutes one of the dominant contributions (or even the dominant one depending on the input for the matrix elements and $\text{SU}(3)_F$ breaking) to the lifetime ratio $\tau(B_s)/\tau(B_d)$.
2. $\text{SU}(3)_F$ breaking corrections to the matrix elements of dimension-six four-quark operators as recently computed in Ref. [96]. These matrix elements were first determined with heavy quark effective theory (HQET) sum rules in Ref. [69] for the case of the B_d meson. It is worthwhile to stress that so far no lattice determination is available in the literature, the most recent estimates date back to proceedings from 2001 [97], while the corresponding publication has never appeared.
3. Consistent determination of dimension-seven four-quark operator contributions. In fact, as it has been pointed out in Ref. [73], previous studies were incorrectly including the effect of some dimension-seven operators, which was actually already accounted for when converting the HQET decay constant to the QCD one.
4. The so-called eye-contractions, which have been computed for the first time in Ref. [96] with HQET sum rules. In this approach the eye-contractions constitute subleading corrections of order α_s to the matrix element of dimension-six four-quark operators and their numerical effect is found to be small.

5. Detailed numerical analysis of the total decay rates of the B_d , B^+ and B_s mesons.
6. Update of all relevant SM parameters, in particular the CKM input.

The paper is structured as follows: in Section 2 we present the main ingredients of the analysis. Specifically, in Section 2.1 we outline the general structure of the HQE for the b -system, in Section 2.2 we describe the status and the updates for the short-distance contributions, while in Section 2.3 we analyse in detail the non-perturbative part of the HQE and the choice of the corresponding input. Our numerical results are discussed in Section 3 and we conclude with a summary and an outlook in Section 4. Finally, all inputs used in our analysis are collected in Appendix A, and we provide the complete expressions for the contribution of dimension-seven four-quark operators in HQET in Appendix B.

2 Theoretical framework

2.1 Effective Hamiltonian and HQE

The most general effective Hamiltonian describing the weak decays of a b -quark, see e.g. Ref. [98], takes the schematic form:

$$\mathcal{H}_{\text{eff}} = \mathcal{H}_{\text{eff}}^{\text{NL}} + \mathcal{H}_{\text{eff}}^{\text{SL}} + \mathcal{H}_{\text{eff}}^{\text{rare}}. \quad (2.1)$$

In the above equation, $\mathcal{H}_{\text{eff}}^{\text{NL}}$ indicates the contribution due to non-leptonic b -quark transitions:

$$\mathcal{H}_{\text{eff}}^{\text{NL}} = \frac{G_F}{\sqrt{2}} \sum_{q_3=d,s} \left[\sum_{q_{1,2}=u,c} \lambda_{q_1 q_2 q_3} \left(C_1(\mu_1) Q_1^{q_1 q_2 q_3} + C_2(\mu_1) Q_2^{q_1 q_2 q_3} \right) - \lambda_{q_3} \sum_{j=3,\dots,6,8} C_j(\mu_1) Q_j^{q_3} \right] + \text{h.c.}, \quad (2.2)$$

where $\lambda_{q_1 q_2 q_3} = V_{q_1 b}^* V_{q_2 q_3}$ and $\lambda_{q_3} = V_{t b}^* V_{t q_3}$ stand for the corresponding CKM factors, $C_i(\mu_1)$ denote the Wilson coefficients of the $\Delta B = 1$ effective operators evaluated at the renormalisation scale $\mu_1 \sim m_b$, while $Q_{1,2}^{q_1 q_2 q_3}$, $Q_j^{q_3}$ ($j = 3, \dots, 6$) and Q_8^q indicate respectively the current-current², the penguin and the chromo-magnetic operators. They have the following expressions:

$$Q_1^{q_1 q_2 q_3} = (\bar{b}^i \Gamma_\mu q_1^i) (\bar{q}_2 \Gamma^\mu q_3^j), \quad Q_2^{q_1 q_2 q_3} = (\bar{b}^i \Gamma_\mu q_1^j) (\bar{q}_2^j \Gamma^\mu q_3^i), \quad (2.3)$$

$$Q_3^{q_3} = (\bar{b}^i \Gamma_\mu q_3^i) \sum_q (\bar{q}^j \Gamma^\mu q^j), \quad Q_4^{q_3} = (\bar{b}^i \Gamma_\mu q_3^j) \sum_q (\bar{q}^j \Gamma^\mu q^i), \quad (2.4)$$

$$Q_5^{q_3} = (\bar{b}^i \Gamma_\mu q_3^i) \sum_q (\bar{q}^j \Gamma_+^\mu q^j), \quad Q_6^{q_3} = (\bar{b}^i \Gamma_\mu q_3^j) \sum_q (\bar{q}^j \Gamma_+^\mu q^i), \quad (2.5)$$

$$Q_8^q = \frac{g_s}{8\pi^2} m_b (\bar{b}^i \sigma^{\mu\nu} (1 - \gamma_5) t_{ij}^a q_3^j) G_{\mu\nu}^a, \quad (2.6)$$

²We emphasise that in our notation $Q_1^{q_1 q_2 q_3}$ is the colour-singlet operator, contrary to e.g. Ref. [98].

with $\Gamma_\mu = \gamma_\mu(1 - \gamma_5)$, $\Gamma_+^\mu = \gamma^\mu(1 + \gamma_5)$ and $\sigma_{\mu\nu} = (i/2)[\gamma_\mu, \gamma_\nu]$. Moreover, in Eqs. (2.3) - (2.6), g_s denotes the strong coupling, $G_{\mu\nu} = G_{\mu\nu}^a t^a$ is the gluon field strength tensor, while $i, j = 1, 2, 3$ and $a = 1, \dots, 8$ label the $SU(3)_c$ indices for fields respectively in the fundamental and in the adjoint representation. A comparison of the values of the corresponding Wilson coefficients for different choices of the scale μ_1 and both at LO- and NLO-QCD [98] is shown in the Appendix in Table 5. The second term in Eq. (2.1) describes the contribution to the effective Hamiltonian due to semileptonic b -quark decays, i.e.

$$\mathcal{H}_{\text{eff}}^{\text{SL}} = \frac{G_F}{\sqrt{2}} \sum_{q=u,c} \sum_{\ell=e,\mu,\tau} V_{qb}^* Q^{q\ell} + \text{h.c.}, \quad (2.7)$$

with

$$Q^{q\ell} = (\bar{b} \Gamma^\mu q) (\bar{\nu}_\ell \Gamma_\mu \ell). \quad (2.8)$$

Finally, $\mathcal{H}_{\text{eff}}^{\text{rare}}$ in Eq. (2.2) encodes the contribution due to suppressed b -quark transitions which are only relevant for the study of rare decays like $B \rightarrow K^{(*)} \gamma$ or $B \rightarrow K \ell^+ \ell^-$. These modes have very small branching fractions which fall out of the current theoretical sensitivity for the lifetimes³. Hence, in the following, the effect of $\mathcal{H}_{\text{eff}}^{\text{rare}}$ is neglected and for brevity we do not show its explicit expression below.

The total decay width of a B_q meson, with mass m_{B_q} and four-momentum p_B reads

$$\Gamma(B_q) = \frac{1}{2m_{B_q}} \sum_X \int_{\text{PS}} (2\pi)^4 \delta^{(4)}(p_B - p_X) |\langle X(p_X) | \mathcal{H}_{\text{eff}} | B_q(p_B) \rangle|^2, \quad (2.9)$$

where PS denotes the phase space integration, and the summation over all possible final states X into which the B meson can decay is performed. Using the optical theorem, $\Gamma(B_q)$ can be related to the discontinuity of the forward scattering matrix element of the time ordered product of the double insertion of the effective Hamiltonian, i.e.

$$\Gamma(B_q) = \frac{1}{2m_{B_q}} \text{Im} \langle B_q | \mathcal{T} | B_q \rangle, \quad (2.10)$$

with the transition operator given by

$$\mathcal{T} = i \int d^4x T \{ \mathcal{H}_{\text{eff}}(x), \mathcal{H}_{\text{eff}}(0) \}. \quad (2.11)$$

The non-local operator in Eq. (2.11) can be evaluated by exploiting the fact that the b -quark is heavy i.e. $m_b \gg \Lambda_{\text{QCD}}$, where the latter defines a typical hadronic scale. In fact, in the framework of the HQE, the b -quark momentum is decomposed as

$$p_b^\mu = m_b v^\mu + k^\mu, \quad (2.12)$$

³E.g. the inclusive radiative decay $B \rightarrow X_s \gamma$ has branching fractions of the order of 10^{-4} , which is considerably below the current accuracy of our analysis.

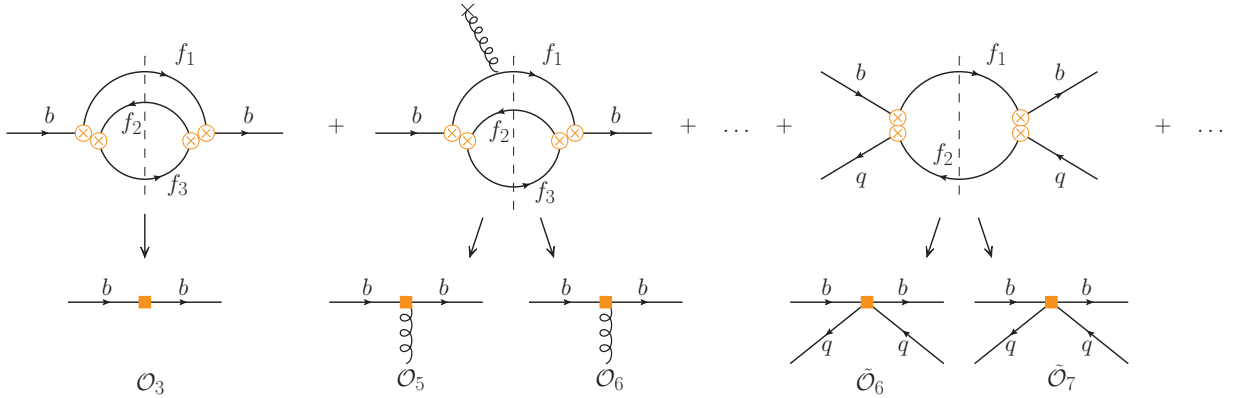


Figure 2: Schematic representation of the HQE for the total decay width of a B -meson. The crossed circles and the full squares denote respectively the insertion of the $\Delta B = 1$ operators Q_i of the effective Hamiltonian, and of the $\Delta B = 0$ operators \mathcal{O}_i and $\tilde{\mathcal{O}}_i$ in the HQE. Note that while the contribution of two-quark operators derives from two-loop diagrams, four-quark operators are generated already at one-loop at LO-QCD. The labels $f_{1,2,3}$ stand for all the possible fermions the b -quark can decay into.

with $v = p_B/m_{B_q}$ denoting the four-velocity of the B -meson, and k representing a residual momentum which accounts for non-perturbative interactions of the b -quark with the light degrees of freedom, i.e. soft gluons and quarks, inside the hadronic state. It thus follows that $k \sim \Lambda_{\text{QCD}}$. Moreover, the heavy b -quark field is parametrised as

$$b(x) = e^{-im_b v \cdot x} b_v(x), \quad (2.13)$$

by factoring out the large component of its momentum and by introducing a rescaled field $b_v(x)$ containing only low oscillation frequencies of the order of k . In fact, this field satisfies

$$iD_\mu b(x) = e^{-im_b v \cdot x} (m_b v_\mu + iD_\mu) b_v(x), \quad (2.14)$$

showing that the action of the covariant derivative $D_\mu = \partial_\mu - ig_s A_\mu^a t^a$ also leads to a large contribution proportional to the heavy quark mass and to a residual term of the order of Λ_{QCD} . Moreover, we recall that the rescaled field $b_v(x)$ is related to HQET field $h_v(x)$, see e.g. Ref. [99], by

$$b_v(x) = h_v(x) + \frac{i\not{D}_\perp}{2m_b} h_v(x) + \mathcal{O}\left(\frac{1}{m_b^2}\right), \quad (2.15)$$

with $D_\perp^\mu = D^\mu - (v \cdot D) v^\mu$. Taking into account Eqs. (2.12) - (2.14), the total decay width in Eq. (2.10) can be systematically expanded in inverse powers of the heavy quark mass, leading to the HQE series. This schematically reads

$$\Gamma(B_q) = \Gamma_3 + \Gamma_5 \frac{\langle \mathcal{O}_5 \rangle}{m_b^2} + \Gamma_6 \frac{\langle \mathcal{O}_6 \rangle}{m_b^3} + \dots + 16\pi^2 \left(\tilde{\Gamma}_6 \frac{\langle \tilde{\mathcal{O}}_6 \rangle}{m_b^3} + \tilde{\Gamma}_7 \frac{\langle \tilde{\mathcal{O}}_7 \rangle}{m_b^4} + \dots \right), \quad (2.16)$$

where Γ_i are short-distance functions which can be computed perturbatively in QCD, i.e.

$$\Gamma_i = \Gamma_i^{(0)} + \frac{\alpha_s}{4\pi} \Gamma_i^{(1)} + \left(\frac{\alpha_s}{4\pi}\right)^2 \Gamma_i^{(2)} + \dots, \quad (2.17)$$

and $\langle \mathcal{O}_i \rangle \equiv \langle B_q | \mathcal{O}_i | B_q \rangle / (2m_{B_q})$ denote the matrix elements of the corresponding $\Delta B = 0$ operators \mathcal{O}_i in the effective theory. Note that at the same order in $1/m_b$, both two- and four-quark operator contributions appear. The latter originate from loop-enhanced diagrams, as reflected by the explicit factor of $16\pi^2$ in Eq. (2.16), and to avoid confusion in the notation, we use a tilde to label them. The diagrammatic representation of Eq. (2.16) is shown in Fig. 2.

2.2 Short-distance contributions

In this section, we give a brief summary of the short-distance contributions, cf. Eq. (2.17), included in our analysis; however, for more details we refer to the recent study [73], where a comprehensive description of the structure of the HQE for the charm sector has been discussed. Note, that the coefficients $\Gamma_i, \tilde{\Gamma}_i$ are analytic functions of the masses of the internal fermions, and in our case, since we only keep non-vanishing the masses of the charm quark and of the tau-lepton⁴, they depend on the two dimensionless mass parameters:

$$\rho = \frac{m_c^2}{m_b^2}, \quad \eta = \frac{m_\tau^2}{m_b^2}. \quad (2.18)$$

The leading contribution to the B -meson total decay width corresponds to the free b -quark decay, obtained by computing the discontinuity, at LO-QCD, of the two-loop diagrams schematically pictured on the top left of Fig. 2. A compact expression for this coefficient takes the form:

$$\Gamma_3 = \Gamma_0 c_3 = \Gamma_0 \left(c_3^{(0)} + \frac{\alpha_s}{4\pi} c_3^{(1)} + \dots \right), \quad (2.19)$$

where

$$\Gamma_0 = \frac{G_F^2 m_b^5}{192\pi^3} |V_{cb}|^2, \quad (2.20)$$

and

$$c_3 = \mathcal{C}_{3,\text{SL}} + 3 C_1^2 \mathcal{C}_{3,11} + 2 C_1 C_2 \mathcal{C}_{3,12} + 3 C_2^2 \mathcal{C}_{3,22} + C_i C_j \mathcal{C}_{3,ij}^P. \quad (2.21)$$

In Eq. (2.21), a summation over all possible non-leptonic and semileptonic modes of the b -quark is implicitly assumed and we have denoted by $\mathcal{C}_{3,ij}^P$ with $i = 1, 2$ and $j = 3, \dots, 6, 8$ the contribution due to the mixed insertion of the current-current and of the penguin or the chromo-magnetic operators. Remarkably, for semileptonic modes even α_s^3 corrections have been computed by now [100, 101], however, as the accuracy for non-leptonic modes reaches only NLO-QCD, we perform our analysis consistently at this order and do not include the new

⁴Since $m_s^2/m_b^2 \approx m_\mu^2/m_b^2 \sim 0.05\%$, the effect of non-vanishing s -quark and μ -lepton masses to the short-distance coefficients is far below the current theoretical accuracy and hence can be safely neglected. However, we must include strange quark mass corrections in the non-perturbative input, where these effects are much more pronounced, in order to account for $\text{SU}(3)_F$ breaking.

results for $\mathcal{C}_{3,SL}$. Moreover, following a common counting adopted in the literature [102, 103], due to the small size of the corresponding Wilson coefficients, the contribution of the penguin and chromo-magnetic operators is in fact treated as a next-to-leading order effect, i.e. $\mathcal{C}_{3,ij}^P = 0$, for $j = 3, \dots, 6, 8$ at LO-QCD. The analytic expressions for $\mathcal{C}_{3,11}$, $\mathcal{C}_{3,22}$, and $\mathcal{C}_{3,SL}$ can be easily extracted from Ref. [104], where the computation has been performed for three different final state masses, while those for $\mathcal{C}_{3,12}$ are derived from the results presented in Ref. [105] in the case of the $b \rightarrow c\bar{c}s$ transition, and in Ref. [106] for the remaining modes. Finally $\mathcal{C}_{3,ij}^P$ are taken from Ref. [105].

At order $1/m_b^2$, the short-distance coefficients are obtained by computing the discontinuity of two-loop diagrams, as the one in the center of Fig. 2, and by taking into account the expansion of the dimension-three matrix element. The corresponding contribution can be schematically written as

$$\Gamma_5 \frac{\langle \mathcal{O}_5 \rangle}{m_b^2} = \Gamma_0 \left[c_\pi \frac{\langle \mathcal{O}_\pi \rangle}{m_b^2} + c_G \frac{\langle \mathcal{O}_G \rangle}{m_b^2} \right], \quad (2.22)$$

where the matrix elements of the kinetic and chromo-magnetic operators, see Eqs. (2.37), (2.38)⁵, are discussed in Section 2.3. In our analysis, again for consistency, we include the coefficients c_π and c_G only at LO-QCD, since α_s corrections have so far been determined only for the semileptonic channels [107]. At this order, the contribution of the kinetic operator is equal to the one of dimension-three up to a numerical factor, i.e. $c_\pi = -c_3^{(0)}/2$, while the coefficient c_G can be decomposed as

$$c_G = \mathcal{C}_{G,SL} + 3 C_1^2 \mathcal{C}_{G,11} + 2 C_1 C_2 \mathcal{C}_{G,12} + 3 C_2^2 \mathcal{C}_{G,22}, \quad (2.23)$$

here again a summation over all the b -quark modes is assumed. The expressions for the non-leptonic channels $\mathcal{C}_{G,ij}$ can be found e.g. in the Appendix of Ref. [92], however originally computed in Refs. [108–110], while the semileptonic coefficient $\mathcal{C}_{G,SL}$ is obtained using the general result for two different final state masses presented e.g. in the Appendix of Ref. [111], and first determined in Refs. [112, 113].

At order $1/m_b^3$, both two- and four-quark operators contribute⁶, see respectively the second and third diagram on the top line of Fig. 2. For the former, we can compactly write

$$\Gamma_6 \frac{\langle \mathcal{O}_6 \rangle}{m_b^3} = \Gamma_0 c_{\rho D} \frac{\langle \mathcal{O}_D \rangle}{m_b^3}, \quad (2.24)$$

where the matrix element of the Darwin operator is defined in Eq. (2.39), while the corresponding short-distance coefficient can be decomposed as:

$$c_{\rho D} = \mathcal{C}_{\rho D,SL} + 3 C_1^2 \mathcal{C}_{\rho D,11} + 2 C_1 C_2 \mathcal{C}_{\rho D,12} + 3 C_2^2 \mathcal{C}_{\rho D,22}, \quad (2.25)$$

⁵Note that with a little abuse of notation, we denote by chromo-magnetic operators both Q_8^{g3} and \mathcal{O}_G . However, as they arise respectively in the $\Delta B = 1$ and $\Delta B = 0$ effective theory, it should be clear from the context to which one we actually refer.

⁶We stress that, by using the equations of motion for the gluon field strength tensor, the dimension-six operator basis can be also written in terms of four-quark operators only, see Section 2.3.

summing again over all b -quark decay modes. Also in this case, the accuracy in our analysis reaches only LO-QCD, as this is the order at which the non-leptonic contributions are known; for the semileptonic decays the coefficient of the Darwin operator has been first computed in Ref. [114], while NLO-QCD corrections have been recently determined in Ref. [115–117]. The complete expressions of $\mathcal{C}_{\rho_D,ij}$ for all non-leptonic channels have been obtained recently in Refs. [92–94], while the coefficient $\mathcal{C}_{\rho_D,SL}$ can be read off the general results for the case of two different final state masses presented e.g. in Refs. [117, 118]. In this respect, it is worth emphasising that contrary to the naive expectation, the coefficient of the Darwin operator is found to be sizeable; more precisely, it results to be one order of magnitude larger than the corresponding ones at dimension-five. However, as it has been shown in detail e.g. in Ref. [92], this actually follows from an accidental suppression of the dimension-five coefficients, and not from an abnormal enhancement of the Darwin term. Therefore, the contribution of the Darwin operator, neglected in previous phenomenological studies, turns out to be an important ingredient for the theoretical prediction of the B -meson lifetimes, see Section 3.

The short-distance coefficients due to four-quark operators are obtained by computing, at LO-QCD, the discontinuity of the one-loop diagrams showed in Fig. 3, corresponding respectively to the weak annihilation (WA), Pauli interference (PI), and weak-exchange (WE) topologies, see e.g. Refs. [67, 119] for results including the charm quark mass dependence. Their contribution, at dimension-six, can be schematically written as

$$16\pi^2 \tilde{\Gamma}_6 \frac{\langle \tilde{\mathcal{O}}_6 \rangle}{m_b^3} = \Gamma_0 \left[A_{i,q_1q_2}^{\text{WE}} \frac{\langle \tilde{\mathcal{O}}_i^{q_3} \rangle}{m_b^3} + A_{i,q_1q_3}^{\text{PI}} \frac{\langle \tilde{\mathcal{O}}_i^{q_2} \rangle}{m_b^3} + A_{i,q_2q_3}^{\text{WA}} \frac{\langle \tilde{\mathcal{O}}_i^{q_1} \rangle}{m_b^3} + A_{i,q_1\ell}^{\text{WA}} \frac{\langle \tilde{\mathcal{O}}_i^{q_1} \rangle}{m_b^3} \right], \quad (2.26)$$

where $i = 1, \dots, 4$ and a sum over all possible final states, following the notation in Eq. (2.2), is implied. Again, we refer to Section 2.3 for a discussion of the matrix elements of the corresponding four-quark operators. Moreover, Eq. (2.26) shows that, contrary to the corrections described so far, now differences in the contributions to specific B_q -mesons arise not only because of different states in the matrix elements, but also due to different short-distance coefficients. In light of this and of the formal loop enhancement with respect to two-quark operators, the effect of four-quark operators was expected to give the dominant correction to the total widths and in particular to the lifetime ratios, see e.g. Refs. [67, 119]. The complete expressions for $A_{i,q_1q_2}^{\text{WE}}$ and $A_{i,q_1q_3}^{\text{PI}}$ up to NLO-QCD corrections, and including also the effect of mixed tree-penguin contributions, have been computed in Ref. [120] for four-quark operators defined in HQET⁷. The results for $A_{i,q_2q_3}^{\text{WA}}$ can be obtained, by means of a Fierz transformation, from the corresponding ones for $A_{i,q_1q_2}^{\text{WE}}$ replacing $C_1 \leftrightarrow C_2$. For semileptonic modes, the coefficients $A_{i,q_1\ell}^{\text{WA}}$ have been determined in Ref. [122].

Finally, at order $1/m_b^4$, only the LO-QCD short-distance coefficients of the four-quark operators are known in the literature. They were determined in Refs. [68, 123] for operators defined in QCD⁸ and also in Ref. [122] for the HQET ones. The corresponding contribution to the

⁷For the case of QCD operators see Refs. [120, 121].

⁸We note that while comparing our results with the ones presented in Refs. [68, 123], we have actually found some inconsistencies in their expressions and communicated this to the authors.

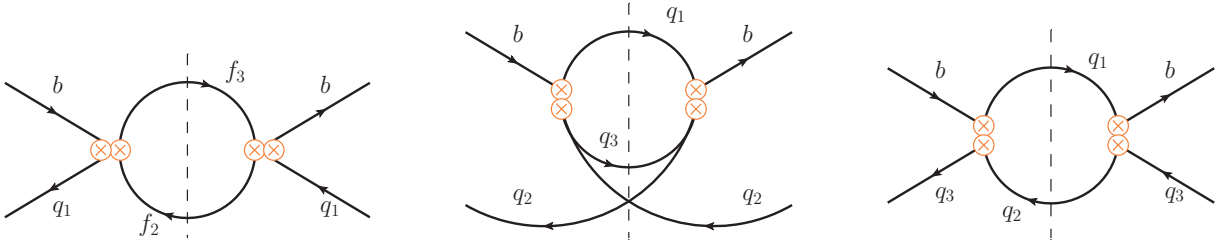


Figure 3: Diagrams corresponding, from left to right, to the WA, PI and WE topology.

total decay width schematically reads

$$16\pi^2 \tilde{\Gamma}_7 \frac{\langle \tilde{\mathcal{O}}_7 \rangle}{m_b^4} = \Gamma_0 \left[B_{i,q_1 q_2}^{\text{WE}} \frac{\langle \tilde{P}_i^{q_3} \rangle}{m_b^4} + B_{i,q_1 q_3}^{\text{PI}} \frac{\langle \tilde{P}_i^{q_2} \rangle}{m_b^4} + B_{i,q_2 q_3}^{\text{WA}} \frac{\langle \tilde{P}_i^{q_1} \rangle}{m_b^4} + B_{i,q_1 \ell}^{\text{WA}} \frac{\langle \tilde{P}_i^{q_1} \rangle}{m_b^4} \right], \quad (2.27)$$

where $i = 1, \dots, 18$. We refer to Appendix B for the analytic expressions of the dimension-seven four-quark operator contribution to the WE, PI, and WA topologies in HQET. The dimension-seven four-quark operator basis, together with the relative parametrisation, is briefly discussed in Section 2.3, while more details can be found in Ref. [73].

2.3 Non-perturbative input

In this section we discuss the status and the choice of the non-perturbative input needed in our analysis. These parametrise the matrix elements of the $\Delta B = 0$ operators in the HQE, and hence encode the contribution to the total decay width due to hadronic effects.

For clarity of the presentation, it is convenient to start with the four-quark operators. At order $1/m_b^3$ in the HQE, we consider the following operator basis, already defined in terms of the HQET field $h_v(x) = b_v(x) + \mathcal{O}(1/m_b)$:

$$\tilde{\mathcal{O}}_1^q = (\bar{h}_v \gamma_\mu (1 - \gamma_5) q) (\bar{q} \gamma^\mu (1 - \gamma_5) h_v), \quad (2.28)$$

$$\tilde{\mathcal{O}}_2^q = (\bar{h}_v (1 - \gamma_5) q) (\bar{q} (1 + \gamma_5) h_v), \quad (2.29)$$

$$\tilde{\mathcal{O}}_3^q = (\bar{h}_v \gamma_\mu (1 - \gamma_5) t^a q) (\bar{q} \gamma^\mu (1 - \gamma_5) t^a h_v), \quad (2.30)$$

$$\tilde{\mathcal{O}}_4^q = (\bar{h}_v (1 - \gamma_5) t^a q) (\bar{q} (1 + \gamma_5) t^a h_v). \quad (2.31)$$

The matrix elements of the operators in Eqs. (2.28) - (2.31) are parameterised as [96]

$$\langle B_q | \tilde{\mathcal{O}}_i^q | B_q \rangle = F_q^2(\mu_0) m_{B_q} \tilde{B}_i^q(\mu_0), \quad (2.32)$$

$$\langle B_q | \tilde{\mathcal{O}}_i^{q'} | B_q \rangle = F_q^2(\mu_0) m_{B_q} \tilde{\delta}_i^{q'q}(\mu_0), \quad q \neq q', \quad (2.33)$$

where $\tilde{B}_i^q(\mu_0)$ ⁹ and $\tilde{\delta}_i^{q'q}(\mu_0)$, $i = 1, \dots, 4$, denote, respectively, the Bag parameters and the so-called eye-contractions, evaluated at the renormalisation μ_0 . We emphasise that the eye-contractions correspond to subleading effects of order α_s to the matrix elements, originating

⁹Note that in the literature $\tilde{\mathcal{O}}_{3,4}^q$ are sometimes denoted by $\tilde{T}_{1,2}^q$, and correspondingly $\tilde{B}_{3,4}^q$ by $\epsilon_{1,2}^q$.

from diagrams in which the spectator quark in the B meson and the light quark in the effective operator do not coincide¹⁰. Moreover, $F_q(\mu_0)$ in Eqs. (2.32) - (2.33) labels the HQET decay constant; this is related to the QCD decay constant f_{B_q} , at one-loop accuracy and up to power corrections, by [124, 125]

$$f_{B_q} = \frac{F_q(\mu_0)}{\sqrt{m_{B_q}}} \left[1 + \frac{\alpha_s(\mu_0)}{2\pi} \left(\ln \left(\frac{m_b^2}{\mu_0^2} \right) - \frac{4}{3} \right) + \mathcal{O} \left(\frac{1}{m_b} \right) \right]. \quad (2.34)$$

In vacuum insertion approximation (VIA), the Bag parameters of the colour-singlet operators are equal to one, while those of the colour-octet operators and all the eye-contractions vanish:

$$\tilde{B}_{1,2}^q \stackrel{\text{VIA}}{=} 1, \quad \tilde{B}_{3,4}^q \stackrel{\text{VIA}}{=} 0, \quad \tilde{\delta}_i^{q'q} \stackrel{\text{VIA}}{=} 0. \quad (2.35)$$

The deviation of the non-perturbative input $\tilde{B}_i^q(\mu_0)$ and $\tilde{\delta}_i^{qq'}(\mu_0)$ from their VIA values has been computed within the framework of HQET sum rules. Specifically, the Bag parameters \tilde{B}_i^q were firstly determined in Ref. [69] for the case of the $B^{+,0}$ mesons, while corrections due to the strange quark mass as well as the contribution of the eye-contractions have been obtained in Ref. [96]. Their numerical values are listed in Table 7. Note that throughout this work we assume isospin symmetry, i.e.

$$\tilde{B}_i^u = \tilde{B}_i^d, \quad \tilde{\delta}_i^{us} = \tilde{\delta}_i^{ds}, \quad \tilde{\delta}_i^{su} = \tilde{\delta}_i^{sd}, \quad \tilde{\delta}_i^{ud} = \tilde{\delta}_i^{du}. \quad (2.36)$$

At order $1/m_b^4$, the HQET operator basis is much larger, specifically it includes 18 operators of which 10 local and 8 non-local, obtained from the expansion of the heavy quark field and of the HQET Lagrangian, see e.g. Ref. [99]. Their complete expressions, together with the parametrisation of their matrix elements can be found in Ref. [73]. Here we limit ourselves to stress that the effect of all non-local operators and of some local ones is actually absorbed in the conversion of the HQET decay constant, cf. Eq. (2.34), when also $1/m_b$ corrections are taken into account¹¹. This has been overlooked in previous analyses [122] and only recently clarified in Ref. [73]. In Appendix B, we present the analytic expression for the dimension-seven contribution to the PI, WE and WA topologies in VIA. Note that so far, there is no computation of the dimension-seven Bag parameters available in the literature.

We now turn to discuss the input needed to parametrise the matrix elements of two-quark operators. Up to order $1/m_b^3$ in the HQE, the basis includes the kinetic and chromo-magnetic

¹⁰The eye-contractions with $q = q'$ are in fact included in the Bag parameters \tilde{B}_i^q .

¹¹We stress that in principle the running of the dimension-seven HQET operators should also be taken into account and would lead to a residual effect not included in the QCD decay constant. A detailed study, performed in Ref. [126] for the case of $B - \bar{B}$ mixing, has found this effect to be small i.e. $\sim 5\%$ for running of μ_0 from the scale m_b to 1 GeV. Since we consider $\mu_0 \sim m_b$ and do not run to low scales ~ 1 GeV, we expect even a much smaller effect to the lifetimes and thus we neglect it in our analysis.

operators at dimension-five and the Darwin operator at dimension-six¹². Namely

$$2m_B \mu_\pi^2(B_q) = -\langle B_q | \bar{b}_v(iD_\mu)(iD^\mu)b_v | B_q \rangle, \quad (2.37)$$

$$2m_B \mu_G^2(B_q) = \langle B_q | \bar{b}_v(iD_\mu)(iD_\nu)(-i\sigma^{\mu\nu})b_v | B_q \rangle, \quad (2.38)$$

$$2m_B \rho_D^3(B_q) = \langle B_q | \bar{b}_v(iD_\mu)(iv \cdot D)(iD^\mu)b_v | B_q \rangle. \quad (2.39)$$

Note that following Ref. [127], the operators in Eqs. (2.37) - (2.39) are defined in terms of $b_v(x)$ and not the HQET field $h_v(x)$. Nevertheless, as we have explicitly checked, any differences between these two choices arise only at order $1/m_b^4$. The values of the non-perturbative parameters μ_π^2 , μ_G^2 , and ρ_D^3 for the case of the B^{+0} meson can be determined from fits to the experimental data on inclusive semileptonic $B \rightarrow X_c \ell \bar{\nu}_\ell$ decays. Analyses using moments of the lepton energy and of the invariant hadronic mass distributions were carried out in Refs. [128, 129], and recently in Ref. [130], where also the new N³LO-QCD results for the parton level decay [100, 101] were included. Very recently a new fit [131] has been performed using data on the moments of the dilepton invariant mass distribution reported by the Belle and Belle-II collaborations [132, 133]. Both analyses [130, 131] yield similar results for V_{cb} , the kinetic mass $m_b^{\text{kin}}(1 \text{ GeV})$ and the parameters $\mu_\pi^2(B)$, $\mu_G^2(B)$. However, there appears to be a significant difference for the value of $\rho_D^3(B)$, see Table 6. Interestingly, it turns out that the Darwin operator, which was neglected in all previous analyses of $\tau(B_s)/\tau(B_d)$, see e.g. Refs. [67, 69], actually yields a large or even dominant contribution to this ratio. As the origin of the discrepancy in the numerical value of $\rho_D^3(B)$ is not yet understood, we consider two scenarios for the choice of the parameters m_b^{kin} , $\mu_\pi^2(B)$, $\mu_G^2(B)$, and $\rho_D^3(B)$, as it is summarised in Table 6 of the Appendix. Specifically, we refer to scenario A when using the input from Ref. [130], and to scenario B when using those of Ref. [131].

It is worthwhile to point out that an alternative way to determine ρ_D^3 makes use of the equations of motion (EOM) for the gluon field strength tensor. In fact, taking into account that

$$D^\mu G_{\mu\rho}^a = -g_s \sum_q (\bar{q} \gamma_\rho t^a q), \quad [iD_\mu, [iD^\rho, iD^\mu]] = g_s D_\mu G^{\mu\rho}, \quad (2.40)$$

the matrix element of the Darwin operator can be written up to $1/m_b$ corrections, as

$$-4m_B \rho_D^3(B_q) = g_s^2 \langle B_q | \mathcal{O}_P | B_q \rangle + \mathcal{O}\left(\frac{1}{m_b}\right). \quad (2.41)$$

In Eq. (2.41), we have introduced the penguin operator

$$\mathcal{O}_P = (\bar{h}_v \gamma_\mu t^a h_v) \sum_q (\bar{q} \gamma^\mu t^a q), \quad (2.42)$$

¹²We stress that at dimension-six the basis formally includes also the spin-orbit operator \mathcal{O}_{LS} . However, by adopting definitions in terms of full covariant derivatives (and not the transversal ones), the contribution of \mathcal{O}_{LS} to the total decay width vanishes, for detail see e.g. Ref. [127].

	$\mu = 4.5 \text{ GeV}$		$\mu = 1.0 \text{ GeV}$		$\alpha_s = 1$	
$\rho_D^3 [\text{GeV}^3]$	VIA	HQET	VIA	HQET	VIA	HQET
B^+, B_d	0.029	0.028	0.061	0.059	0.133	0.128
B_s	0.044	0.043	0.092	0.090	0.199	0.195

Table 3: Comparison of the values of $\rho_D^3(B_q)$ obtained using Eqs. (2.41), (2.43), for different choices of the renormalisation scale, and using VIA and HQET sum rules results for the non-perturbative input.

whose matrix element can be parametrised as [96]¹³

$$\langle B_q | \mathcal{O}_P | B_q \rangle = -\frac{2}{9} f_{B_q}^2 m_B^2 \left(\tilde{B}_P^q + \sum_{q' \neq q} \tilde{\delta}_P^{q'q} \right). \quad (2.43)$$

Again, the input \tilde{B}_P^q and $\tilde{\delta}_P^{q'q}$ in Eq. (2.43) denote the corresponding Bag parameters and the eye-contractions also determined for the first time in Ref. [96] within the framework of HQET sum rules. Note that in VIA, Eqs. (2.41), (2.43) lead to the following simplified expression for the Darwin parameter up to power corrections, i.e.

$$\rho_D^3(B_q) \approx \frac{g_s^2}{18} f_{B_q}^2 m_{B_q}. \quad (2.44)$$

A comparison of the values of ρ_D^3 obtained for different choices of the renormalisation scale at which the strong coupling is evaluated, and using both the HQET sum rules and the VIA results for the non-perturbative input in Eq. (2.43), is shown in Table 3. In this respect, two comments are in order. First, HQET sum rules and VIA yield very similar results for ρ_D^3 . Second, it is interesting to observe that setting $\mu \sim m_b$, leads to a value for ρ_D^3 in very good agreement with the one obtained by the fit of Ref. [131], whereas the result given in Ref. [130] is reproduced by setting $\alpha_s \sim 1$, i.e. choosing a very low renormalisation scale.

In order to predict $\Gamma(B_s)$ and $\tau(B_s)/\tau(B_d)$, we also need to fix the size of the largely unknown $\text{SU}(3)_F$ breaking effects in the non-perturbative parameters discussed above. A possible estimate for the value of $\mu_G^2(B_{(s)})$ can be obtained using the spectroscopy relation [134]

$$\mu_G^2(B_{(s)}) \approx \frac{3}{4} \left(M_{B_{(s)}^*}^2 - M_{B_{(s)}}^2 \right), \quad (2.45)$$

¹³Note that by means of Fierz transformations, the matrix element of the penguin operator can be recast in terms of a linear combination of the four-quark operators given in Eqs. (2.28) - (2.31), together with the corresponding ones obtained by replacing $(1 - \gamma_5) \rightarrow (1 + \gamma_5)$. Taking into account parity conservation in QCD and the parametrisation in Eqs. (2.32) - (2.33) leads to an expression analogous to Eq. (2.43) and numerically consistent with it.

which yields

$$\frac{\mu_G^2(B_s)}{\mu_G^2(B)} \simeq \frac{M_{B_s^*}^2 - M_{B_s}^2}{M_{B^*}^2 - M_B^2} \simeq 1.09 \pm 0.05. \quad (2.46)$$

In Eq. (2.46), the values of the mesons masses are taken from Ref. [135] and lead to a vanishing uncertainty. Therefore we have assigned a conservative 50% uncertainty to the deviation from one in order to account for missing power corrections. Recently, the size of the $SU(3)_F$ breaking in μ_G^2 has been estimated using lattice QCD in Refs. [136, 137], indicating larger effects [138]

$$\frac{\mu_G^2(B_s)}{\mu_G^2(B)} \simeq 1.20 \pm 0.10, \quad (2.47)$$

however in agreement with Eq. (2.46) within uncertainties. In the case of the kinetic operator, μ_π^2 can be determined using the spin-averaged masses, see e.g. Ref. [139], leading to [138, 139]

$$\mu_\pi^2(B_s) - \mu_\pi^2(B) \approx (0.04 \pm 0.02) \text{ GeV}^2, \quad (2.48)$$

valid up to power corrections, which are "accounted" by adding again a conservative 50% uncertainty in Eq. (2.48). On the other side, recent lattice QCD estimates [137] again predict somehow larger $SU(3)_F$ breaking effects,

$$\mu_\pi^2(B_s) - \mu_\pi^2(B) \approx (0.11 \pm 0.03) \text{ GeV}^2. \quad (2.49)$$

Finally, the size of the $SU(3)_F$ breaking effects in ρ_D^3 can be estimated using the EOM relation in Eq. (2.44), yielding

$$\frac{\rho_D^3(B_s)}{\rho_D^3(B)} \approx \frac{f_{B_s}^2 m_{B_s}}{f_B^2 m_B} \approx 1.49 \pm 0.25, \quad (2.50)$$

where we have used lattice results for the decay constants [140], see Table 6, and have again assigned additional conservative 50% uncertainty to the deviation from one due to missing power corrections. As one can see, Eq. (2.50) predicts very large $\approx 50\%$ $SU(3)_F$ breaking in ρ_D^3 . An alternative way to estimate $\rho_D^3(B_s)/\rho_D^3(B)$ is based on the sum rules in the heavy quark limit, see e.g. Ref. [139], which leads to

$$\frac{\rho_D^3(B_s)}{\rho_D^3(B)} \simeq \left(\frac{\mu_\pi^2(B_s)}{\mu_\pi^2(B)} \right)^2 \frac{\bar{\Lambda}}{\bar{\Lambda}_s} \approx \begin{cases} 1.05 \pm 0.09 & \text{using Eq. (2.48)}, \\ 1.35 \pm 0.16 & \text{using Eq. (2.49)}, \end{cases} \quad (2.51)$$

with $\bar{\Lambda}_{(s)} = m_{B_{(s)}} - m_b$, and we have used for $\mu_\pi^2(B)$ the value from Ref. [137], as it is more precise than the one from Ref. [131], cf. Table 6. Note that Eq. (2.51) is very sensitive to the $SU(3)_F$ breaking in μ_π^2 , and using the estimate in Eq. (2.48) yields a much smaller value for $\rho_D^3(B_s)/\rho_D^3(B)$ than the result in Eq. (2.50).

As we see from the discussion above, the estimates of the $SU(3)_F$ breaking in the matrix elements of the two-quark operators differ quite sizeably depending on the method used. These differences will strongly affect the lifetime ratio $\tau(B_s)/\tau(B_d)$. Taking into account also the two fits [130, 131], in our analysis we therefore consider the following two scenarios, to cover both extreme cases for $\tau(B_s)/\tau(B_d)$:

- **Scenario A:** Non-perturbative parameters from fit by Ref. [130] (with large value of ρ_D^3) and larger $SU(3)_F$ breaking effects by using Eqs. (2.47), (2.49) and (2.50).
- **Scenario B:** Non-perturbative parameters from fit by Ref. [131] (with small value of ρ_D^3) and smaller $SU(3)_F$ breaking effects by Eqs. (2.46), (2.48) and the first line of (2.51).

A future, more precise determination of these non-perturbative parameters and of the corresponding size of $SU(3)_F$ breaking - either by fits of inclusive semileptonic B and B_s decays or by non-perturbative calculations - is clearly necessary to obtain more insights on the theoretical prediction of $\tau(B_s)/\tau(B_d)$. All the values used in our analysis for the non-perturbative parameters, in correspondence of these two scenarios, are summarised in Table 6.

3 Numerical analysis and results

In this section we present the theoretical predictions for the B -mesons total decay widths, together with their lifetime ratios. All the input used in our analysis are listed in Appendix A. Note that, we consider two scenarios A and B, defined explicitly in the previous section, depending on which input we use for the parameters μ_π^2, μ_G^2 and ρ_D^3 . To be consistent with the results of both fits by Refs. [130] and [131], by default, in our numerical analysis the mass of the b -quark is expressed in the kinetic scheme [141, 142] fixing the cut-off scale $\mu^{\text{cut}} = 1 \text{ GeV}$, while we adopt the $\overline{\text{MS}}$ scheme for the charm quark mass [143], i.e.

$$m_b^{\text{pole}} = m_b^{\text{kin}}(\mu^{\text{cut}}) \left[1 + \frac{4\alpha_s}{3\pi} \left(\frac{4}{3} \frac{\mu^{\text{cut}}}{m_b^{\text{kin}}} + \frac{1}{2} \left(\frac{\mu^{\text{cut}}}{m_b^{\text{kin}}} \right)^2 \right) \right] + \mathcal{O}(\alpha_s^2), \quad (3.1)$$

$$m_c^{\text{pole}} = \overline{m}_c(\overline{m}_c) \left[1 - \frac{\alpha_s}{\pi} \left(\ln \left(\frac{\overline{m}_c^2}{\mu^2} \right) - \frac{4}{3} \right) \right] + \mathcal{O}(\alpha_s^2). \quad (3.2)$$

In order to understand the size of each of the contributions to the HQE, in the following we show the partial decomposition for all the five observables considered. Note that below we set $m_b^{\text{kin}}(1 \text{ GeV}) = 4.573 \text{ GeV}$, and use the notation $q = u, d$, and $\tilde{\delta}_i^{qq} \equiv \tilde{\delta}_i^{ud} = \tilde{\delta}_i^{du}$. For the three total widths we obtain:

$$\begin{aligned} \Gamma(B^+) = \Gamma_0 & \left[\underbrace{5.97}_{\text{LO}} - \underbrace{0.44}_{\Delta\text{NLO}} - 0.14 \frac{\mu_\pi^2(B)}{\text{GeV}^2} - 0.24 \frac{\mu_G^2(B)}{\text{GeV}^2} - 1.35 \frac{\rho_D^3(B)}{\text{GeV}^3} \right. \\ & - \underbrace{(0.143 + 0.194)}_{\text{LO}} \tilde{B}_1^q + \underbrace{(0.023 - 0.014)}_{\Delta\text{NLO}} \tilde{B}_2^q + \underbrace{(2.29 + 0.40)}_{\text{LO}} \tilde{B}_3^q \\ & + \underbrace{(0.00)}_{\text{LO}} - \underbrace{0.05}_{\Delta\text{NLO}} \tilde{B}_4^q - 0.01 \tilde{\delta}_1^{qq} + 0.01 \tilde{\delta}_2^{qq} - 0.74 \tilde{\delta}_3^{qq} + 0.78 \tilde{\delta}_4^{qq} \\ & \left. - 0.01 \tilde{\delta}_1^{sq} + 0.01 \tilde{\delta}_2^{sq} - 0.69 \tilde{\delta}_3^{sq} + 0.77 \tilde{\delta}_4^{sq} + \underbrace{0.03}_{\text{dim. 7}} \right], \quad (3.3) \end{aligned}$$

$$\begin{aligned}
\Gamma(B_d) = \Gamma_0 & \left[\underbrace{5.97}_{\text{LO}} - \underbrace{0.44}_{\Delta\text{NLO}} - 0.14 \frac{\mu_\pi^2(B)}{\text{GeV}^2} - 0.24 \frac{\mu_G^2(B)}{\text{GeV}^2} - 1.35 \frac{\rho_D^3(B)}{\text{GeV}^3} \right. \\
& - \left(\underbrace{0.012}_{\text{LO}} + \underbrace{0.022}_{\Delta\text{NLO}} \right) \tilde{B}_1^q + \left(\underbrace{0.012}_{\text{LO}} + \underbrace{0.020}_{\Delta\text{NLO}} \right) \tilde{B}_2^q - \left(\underbrace{0.74}_{\text{LO}} + \underbrace{0.03}_{\Delta\text{NLO}} \right) \tilde{B}_3^q \\
& + \left(\underbrace{0.78}_{\text{LO}} - \underbrace{0.01}_{\Delta\text{NLO}} \right) \tilde{B}_4^q - 0.14 \tilde{\delta}_1^{qq} + 0.02 \tilde{\delta}_2^{qq} - 2.29 \tilde{\delta}_3^{qq} + 0.00 \tilde{\delta}_4^{qq} \\
& \left. - 0.01 \tilde{\delta}_1^{sq} + 0.01 \tilde{\delta}_2^{sq} - 0.69 \tilde{\delta}_3^{sq} + 0.78 \tilde{\delta}_4^{sq} + \underbrace{0.00}_{\text{dim. } 7} \right], \tag{3.4}
\end{aligned}$$

$$\begin{aligned}
\Gamma(B_s) = \Gamma_0 & \left[\underbrace{5.97}_{\text{LO}} - \underbrace{0.44}_{\Delta\text{NLO}} - 0.14 \frac{\mu_\pi^2(B_s)}{\text{GeV}^2} - 0.24 \frac{\mu_G^2(B_s)}{\text{GeV}^2} - 1.35 \frac{\rho_D^3(B_s)}{\text{GeV}^3} \right. \\
& - \left(\underbrace{0.016}_{\text{LO}} + \underbrace{0.034}_{\Delta\text{NLO}} \right) \tilde{B}_1^s + \left(\underbrace{0.018}_{\text{LO}} + \underbrace{0.033}_{\Delta\text{NLO}} \right) \tilde{B}_2^s - \left(\underbrace{1.03}_{\text{LO}} - \underbrace{0.03}_{\Delta\text{NLO}} \right) \tilde{B}_3^s \\
& + \left(\underbrace{1.16}_{\text{LO}} - \underbrace{0.07}_{\Delta\text{NLO}} \right) \tilde{B}_4^s - 0.23 \tilde{\delta}_1^{qs} + 0.05 \tilde{\delta}_2^{qs} + 2.32 \tilde{\delta}_3^{qs} + 1.17 \tilde{\delta}_4^{qs} + \underbrace{0.00}_{\text{dim. } 7} \left. \right], \tag{3.5}
\end{aligned}$$

where the size of the NLO-QCD corrections to the partonic level decay and to the coefficients of the dimension-six four-quark operators has been explicitly indicated. As we can see, the dominant contribution to Eqs. (3.3) - (3.5) is given by the total width of the b -quark, while power and radiative corrections appear to be under control and are of order of few percents. For the leading term Γ_b , as it has already been mentioned above, even N³LO-QCD corrections to semileptonic decays are known; in the scheme $m_b^{\text{kin}}(1 \text{ GeV})$ and $\overline{m}_c(2 \text{ GeV})$, the authors of Ref. [100] find respectively -8.7% at NLO, -1.8% at NNLO and -0.03% at N³LO, meaning that higher order effects are negative and very small. NLO-QCD corrections to Γ_b in the total width amount to $\sim -7.4\%$, but for the actual size of higher order effects the complete computation of α_s^2 corrections due to non-leptonic b -quark decays is needed. Looking at the effect of the two-quark operators, it might come as surprising that the coefficient of ρ_D^3 is about one order of magnitude larger than those in front of μ_π^2 and μ_G^2 . However, this follows from an accidental suppression of the dimension-five contribution, more than from an enhancement of the Darwin term, hence we do not expect problems with the convergence of the HQE when including higher power corrections. The series, in the case of inclusive semileptonic B -decays, where $1/m_b^4$ corrections to two-quark operators are known, is in fact well-behaving, see e.g. the discussion in Ref. [92]. Moreover, we refer to the latter for details on the size of the coefficient of the Darwin operator. Assuming the absence of unexpected enhancements at higher orders, in our study we conservatively add extra 15% uncertainty to the dimension-six contribution in order to account for missing $1/m_b^4$ corrections. Concerning the effect of four-quark operators, we find, as expected, that the most sizeable shift derives from the PI topology, which constitutes the dominant contribution to the total width of the B^+ meson,

whereas it enters $\Gamma(B_d)$ and $\Gamma(B_s)$ only through the eye-contractions. On the other side, the WE diagrams, which represent the dominant topologies for the B_d and B_s mesons, are affected by helicity suppression at LO-QCD and lead only to a small contribution. Furthermore, we see that while the operators \tilde{O}_3^q and \tilde{O}_4^q have generally the largest coefficients, the corresponding Bag parameters are very small, not more than few percents in magnitude, and they completely vanish in VIA. On the contrary, the operators \tilde{O}_1^q and \tilde{O}_2^q have smaller coefficients but larger Bag parameters of the order of one. Regarding the size of the NLO-QCD corrections to spectator effects, they turn out to be very sizeable, particularly in the case of $\Gamma(B^+)$, therefore the computation of higher order corrections is of great relevance and should be addressed in the future. On the other side, the contribution of the eye-contractions is generally found to be negligible, if one uses the HQET sum rule predictions for the corresponding matrix elements, see Ref. [96]. Dimension-seven corrections are also relatively small in $\Gamma(B^+)$, where they are dominated by the PI topology, and almost negligible for the total width of the B_d and B_s mesons, again because of the helicity suppression in WE. Finally, along the same line as for the two-quark operator contribution, also in this case we add extra 15% uncertainty to the dimension-seven correction in order to account for missing higher order terms. The theoretical predictions for the lifetime ratios are obtained from Eq. (1.2) using as input the experimental value for $\tau(B^+)$ and $\tau(B_s)$ in order to cancel the dependence on the dimension-three contribution. We respectively obtain

$$\begin{aligned} \tau(B^+)/\tau(B_d) = & 1 + 0.059 \tilde{B}_1^q + 0.005 \tilde{B}_2^q - 0.674 \tilde{B}_3^q + 0.160 \tilde{B}_4^q \\ & - 0.025 \tilde{\delta}_1^{qq} + 0.002 \tilde{\delta}_2^{qq} + 0.591 \tilde{\delta}_3^{qq} - 0.152 \tilde{\delta}_4^{qq} - \underbrace{0.007}_{\text{dim. 7}}, \end{aligned} \quad (3.6)$$

$$\begin{aligned} \tau(B_s)/\tau(B_d) = & 1 + 0.026 [\mu_\pi^2(B_s) - \mu_\pi^2(B)] + 0.043 [\mu_G^2(B_s) - \mu_G^2(B)] \\ & + 0.244 [\rho_D^3(B_s) - \rho_D^3(B)] \\ & - 0.0061 \tilde{B}_1^q + 0.0058 \tilde{B}_2^q - 0.1382 \tilde{B}_3^q + 0.1385 \tilde{B}_4^q \\ & + 0.0091 \tilde{B}_1^s - 0.0093 \tilde{B}_2^s + 0.1812 \tilde{B}_3^s - 0.1967 \tilde{B}_4^s \\ & - 0.0258 \tilde{\delta}_1^{qq} + 0.0041 \tilde{\delta}_2^{qq} + 0.4136 \tilde{\delta}_3^{qq} + 0.0001 \tilde{\delta}_4^{qq} \\ & - 0.0020 \tilde{\delta}_1^{qs} + 0.0022 \tilde{\delta}_2^{qs} - 0.1253 \tilde{\delta}_3^{qs} + 0.1403 \tilde{\delta}_4^{qs} \\ & + 0.0417 \tilde{\delta}_1^{sq} - 0.0095 \tilde{\delta}_2^{sq} - 0.4190 \tilde{\delta}_3^{sq} - 0.2110 \tilde{\delta}_4^{sq} - \underbrace{7 \times 10^{-6}}_{\text{dim. 7}}. \end{aligned} \quad (3.7)$$

From Eq. (3.6) and taking into account the values of the Bag parameters, we see that the dominant correction to $\tau(B^+)/\tau(B_d)$ is given by the operators \tilde{O}_1^u and \tilde{O}_3^u because of the large PI contribution in $\Gamma(B^+)$, whereas the effect of the remaining non-perturbative input is much smaller. Therefore, in order to improve the theoretical prediction for $\tau(B^+)/\tau(B_d)$, both the computation of NNLO corrections to the four-quark operators and a more precise

Observable	HQE Scenario A	HQE Scenario B	Exp. value
$\Gamma(B^+)[\text{ps}^{-1}]$	$0.563^{+0.106}_{-0.065}$	$0.576^{+0.107}_{-0.067}$	0.6105 ± 0.0015
$\Gamma(B_d)[\text{ps}^{-1}]$	$0.615^{+0.108}_{-0.069}$	$0.627^{+0.110}_{-0.070}$	0.6583 ± 0.0017
$\Gamma(B_s)[\text{ps}^{-1}]$	$0.597^{+0.109}_{-0.069}$	$0.625^{+0.110}_{-0.071}$	0.6596 ± 0.0026
$\tau(B^+)/\tau(B_d)$	$1.0855^{+0.0232}_{-0.0219}$	$1.0851^{+0.0230}_{-0.0217}$	1.076 ± 0.004
$\tau(B_s)/\tau(B_d)$	$1.0279^{+0.0113}_{-0.0113}$	$1.0032^{+0.0063}_{-0.0063}$	0.998 ± 0.005

Table 4: Theoretical predictions for the B -meson total decay widths and their lifetimes ratios, based on the HQE and in correspondence of the scenarios A and B as discussed in the text. The quoted uncertainties include the variation of all the input parameters and of the renormalisation scales μ_1 and μ_0 , together with the estimate of higher order power corrections, all combined in quadrature. The respective experimental determinations are also shown.

determination of the corresponding Bag parameters would be highly desirable. For the ratio $\tau(B_s)/\tau(B_d)$, the situation is less trivial. The theoretical prediction for this observable is entirely driven by the size of the $SU(3)_F$ breaking effects in the non-perturbative matrix elements of the B_s and B_d mesons. For both of them the dominant contribution from the four-quark operators originates from the WE topology. However, the latter is extremely suppressed, because of, on one side, the specific combination of the corresponding $\Delta B = 1$ Wilson coefficients, and, on the other side, the helicity suppression affecting these diagrams. In light of this, the role of two-quark operators becomes crucial. Depending on the numerical input values we are using for μ_π^2 , μ_G^2 and ρ_D^3 , the dimension-five two-quark operators can give contributions of up to several per mille to $\tau(B_s)/\tau(B_d)$, while the Darwin operator can even contribute with up to two per cent, a result absolutely unexpected a priori.

When varying all the input parameters within their uncertainties, as listed in Appendix A, we obtain the results shown in Table 4 and Fig. 4. In addition, to demonstrate the size of the individual contribution of different parameters to the error budget for the decay widths and lifetime ratios, we show the corresponding pie charts in Fig. 5. We find that the main source of uncertainty to the decay widths comes from the variation of the scale μ_1 , and that "subdominant" contributions are due to the b - and c -quark masses and $|V_{cb}|^2$. In the case of the lifetime ratio $\tau(B^+)/\tau(B_d)$ the error budget is dominated by the value of the Bag parameters and by the variation of the scale μ_0 . In this regard, as already stressed above, an independent computation by lattice QCD of the matrix elements of the dimension-six four-quark operators and the complete determination of the NNLO-QCD corrections to the corresponding coefficients might be very helpful in reducing the relative uncertainty. The lifetime ratio $\tau(B_s)/\tau(B_d)$ is very sensitive to the parameter $\rho_D^3(B)$, because of its large coefficient, and to the size of the

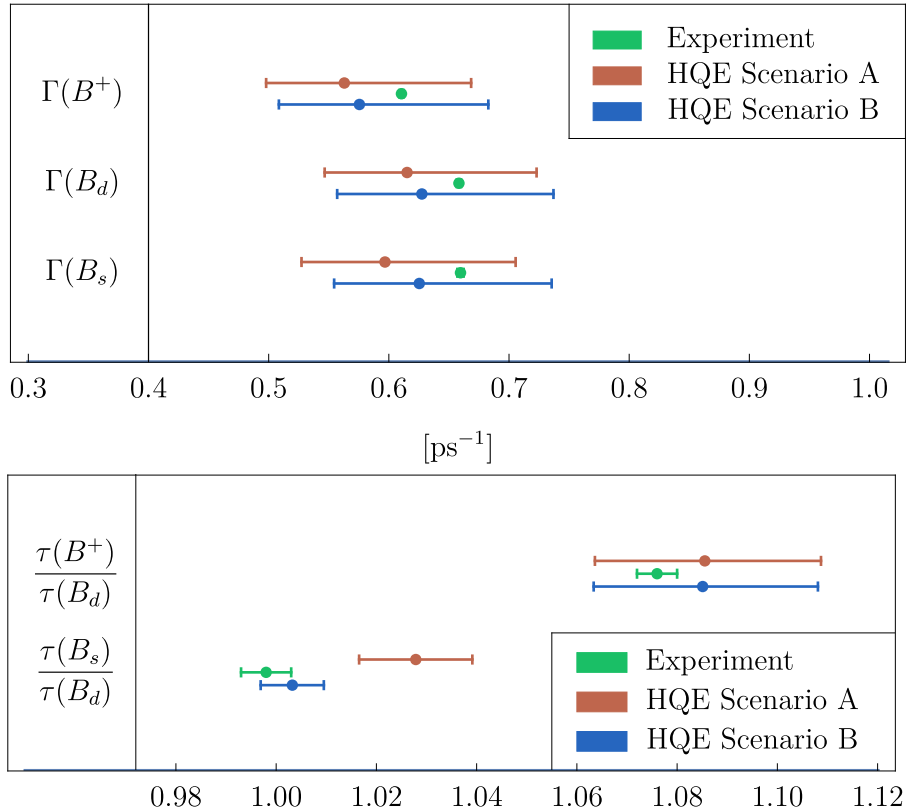


Figure 4: Summary of the HQE predictions for B -meson lifetimes and their ratios within scenarios A and B defined in Section 2.3. The theoretical determinations are compared with the corresponding experimental data, all the respective values are summarised in Table 4.

$SU(3)_F$ breaking effects in all the non-perturbative input. Unfortunately the numerical values of these non-perturbative matrix elements are currently badly known. Therefore we consider two different scenarios for the parameters $m_b^{\text{kin}}(1\text{GeV})$, μ_π^2 , μ_G^2 , and ρ_D^3 and we observe that both sets of input yield very similar results for all observables, except for $\tau(B_s)/\tau(B_d)$.

Within uncertainties all our predictions are found to be in perfect agreement with the corresponding experimental data, again, with the exception of $\tau(B_s)/\tau(B_d)$, where it appears to be some tension within Scenario A. Finally, we have explicitly checked that computing the lifetime ratios entirely within the HQE, i.e. without using the experimental values for $\tau(B^+)$ and $\tau(B_s)$ as input, leads to very similar results as the ones stated in Table 4 and in Fig. 4, although with slightly larger uncertainties.

4 Conclusion

With the present work, we have updated the SM prediction, within the framework of the HQE, for the decay width of the B^+ , B_d , and B_s mesons, together with the lifetime ratios $\tau(B^+)/\tau(B_d)$ and $\tau(B_s)/\tau(B_d)$. Compared to the previous study [69], we have, in addition, included the contribution of the Darwin operator, which is sizeable and crucially affects the

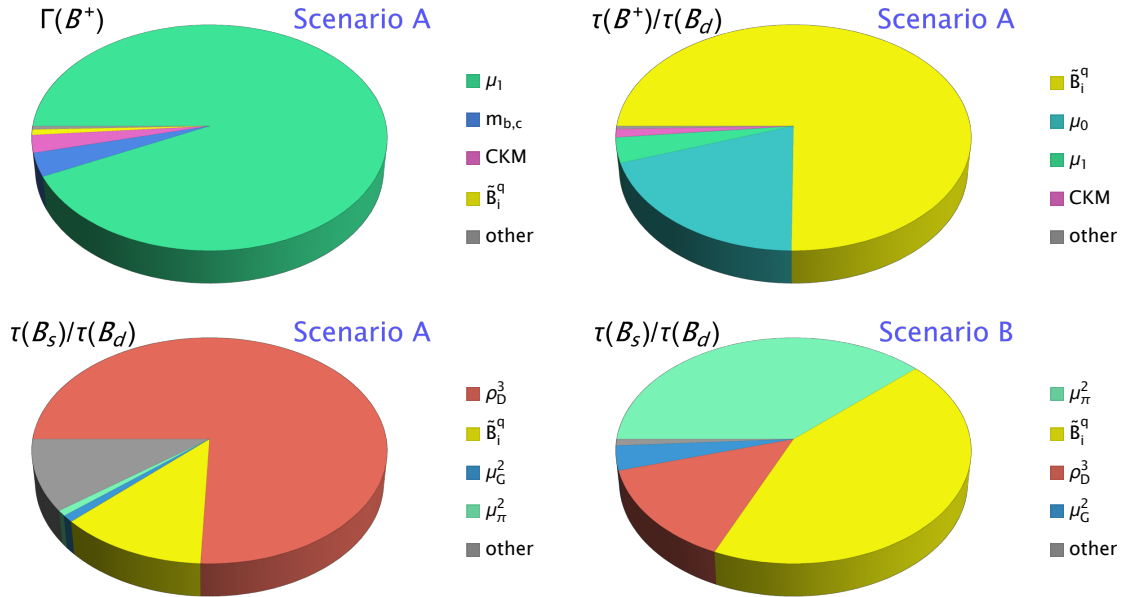


Figure 5: Size of the individual contributions to the error budget for the decay widths and lifetime ratios. Since we combine all uncertainties in quadrature, the values shown here are defined as $(\Delta_i f / \Delta_T f)^2$, where $\Delta_i f$ denotes an individual uncertainty due to the i parameter, and $\Delta_T f$ is the total error. Among the decay widths, here we display only $\Gamma(B^+)$, since the pie charts for $\Gamma(B_d)$ and $\Gamma(B_s)$ are very similar with even smaller effects due to the Bag parameters. There are also no visible differences between scenarios A and B for the decay widths. For $\tau(B_s)/\tau(B_d)$ we show the error budget in both the scenarios A and B, while for $\tau(B^+)/\tau(B_d)$ we present only the scenario A, since the scenario B yields almost the same picture.

ratio $\tau(B_s)/\tau(B_d)$, corrections to the Bag parameters due to the strange quark mass, eye-contractions, and the consistent dimension-seven four-quark operator contribution in HQET. To our best knowledge, we perform the first comprehensive study of the total decay rates of the B_d , B^+ and B_s mesons. Our theory predictions for the latter agree well with experiment, albeit with large uncertainties, see Table 4. From a phenomenological point of view, this implies that huge BSM contributions of the order of 10% to the total decay rate can currently not be excluded by these observables. For the ratio $\tau(B^+)/\tau(B_d)$, our prediction is in a very good agreement with the experimental value. Compared to the experimental relative precision of 4 per mille, we find a theory uncertainty of around 2 per cent. In the case of $\tau(B_s)/\tau(B_d)$, the situation is, however, more complicated. This ratio is extremely sensitive to the value of $\rho_D^3(B)$ and to the size of $SU(3)_F$ breaking in the parameter $\mu_\pi^2(B)$, $\mu_G^2(B)$ and $\rho_D^3(B)$. Unfortunately, neither of these non-perturbative inputs are currently well known. Specifically, we find excellent agreement of $\tau(B_s)/\tau(B_d)$ with the data when using the fit results for $\mu_\pi^2(B)$, $\mu_G^2(B)$ and $\rho_D^3(B)$ from Ref. [131] and estimates of $SU(3)_F$ breaking from spectroscopy relations. In that case, we also find both the experimental and theoretical precision to be of the order of 6

per mille. However, if we use the fit results for $\mu_\pi^2(B)$, $\mu_G^2(B)$ and $\rho_D^3(B)$ from Ref. [130] and the $SU(3)_F$ breaking from lattice QCD and from EOM relation for ρ_D^3 , our theory prediction for $\tau(B_s)/\tau(B_d)$ lies above the experimental value, and we find also a theoretical uncertainty almost twice as large as the experimental one.

Leaving this issue with ρ_D^3 aside for the moment, we nevertheless come to the conclusion that the HQE works very well for decays of the lightest B -mesons, and thus provides an additional opportunity for accurate tests of the Standard Model and for constraining the parameter space of certain BSM models. In order to pursue these two the goals, several possible improvements to the theoretical prediction of B -meson lifetimes and their ratios would very desirable in the future. Specifically:

- Clarification of the difference in the numerical value of $\rho_D^3(B)$ obtained in the fits performed in Ref. [130] and Ref. [131]. In this respect, it would probably be worthwhile to perform a combined fit using all sets of experimental data on semileptonic B -meson decays available in the literature.
- Extraction of the matrix elements of the kinetic, the chromo-magnetic and the Darwin operators for the B_s meson from a fit to future experimental data on inclusive semileptonic B_s decays. This will allow for a more robust determination of the size of the $SU(3)_F$ breaking effects in the corresponding non-perturbative parameters. In parallel, more precise non-perturbative studies of these parameters either with lattice QCD or with sum rules would be very desirable.
- Computation of dimension-seven two-quark operator contribution to non-leptonic b -quark decays, $\Gamma_7^{(0)}$. This might in fact provide a very important correction for the theoretical determination of $\tau(B_s)/\tau(B_d)$ in the light of crucial role played by the Darwin operator, as discussed in Section 3.
- Computation of α_s^2 corrections to the non-leptonic decays of the free b -quark, $\Gamma_3^{(2)}$. In particular, this will lead to a reduction of the theory uncertainty in the total decay widths due to the renormalisation scale variation. A first step in that direction has been done in Ref. [144].
- Computation of α_s^2 corrections to the coefficient of the dimension-six four-quark operators, $\tilde{\Gamma}_6^{(2)}$. This may considerably improve the theoretical predictions for the lifetime ratios, since the corresponding NLO-QCD corrections have been found to be quite sizeable.
- Computation of α_s corrections to the coefficient of the dimension-seven four-quark operators, $\tilde{\Gamma}_7^{(1)}$. In fact, the additional gluon contribution will lift the helicity suppression affecting the WE and WA diagrams.

- First lattice determination of the matrix elements of the dimension-six four-quark operators, in order to have a cross-check of the corresponding HQET sum rules results, and in particular of the small size of eye-contractions.
- First non-perturbative determination of the matrix elements of the dimension-seven four-quark operators. In fact, possible sizeable deviations from VIA in the corresponding Bag parameters may lift the helicity suppression affecting the WE and WA diagrams already at LO-QCD.

Acknowledgements

The authors would like to thank Martin Beneke, Gerhard Buchalla, Matteo Fael, Thomas Mannel, Daniel Moreno, Uli Nierste, Alexey Petrov, Alexei Pivovarov and Keri Vos for helpful discussions and Matthew Kirk for providing an older version of Fig. 1. The work of M.L.P. is financed by the BMBF project *Theoretische Methoden für LHCb und Belle II* (Förderkennzeichen 05H21PSCLA/ErUM-FSP T04). This research has benefited from the support of the Munich Institute for Astro- Particle and BioPhysics (MIAPbP), which is funded by the Deutsche Forschungsgemeinschaft (DFG, German Research Foundation) under Germany Excellence Strategy – EXC-2094 – 390783311.

A Numerical input

We use five-loop running for $\alpha_s(\mu)$ [145] with five active flavours at the scale $\mu \sim m_b$, and the most recent value [135]

$$\alpha_s(M_Z) = 0.1179 \pm 0.0010. \quad (\text{A.1})$$

The masses of B -mesons are known very precisely [135]

$$m_{B^+} = 5.27934 \text{ GeV}, \quad m_{B_d} = 5.27965 \text{ GeV}, \quad m_{B_s} = 5.36688 \text{ GeV}. \quad (\text{A.2})$$

For the CKM matrix elements we adopt the standard parametrisation in terms of $\theta_{12}, \theta_{13}, \theta_{22}, \delta$ and use as input [146] (online update)

$$|V_{us}| = 0.22500^{+0.00024}_{-0.00021}, \quad (\text{A.3})$$

$$\frac{|V_{ub}|}{|V_{cb}|} = 0.08848^{+0.00224}_{-0.00219}, \quad (\text{A.4})$$

$$|V_{cb}| = 0.04145^{+0.00035}_{-0.00061}, \quad (\text{A.5})$$

$$\delta = (65.5^{+1.3}_{-1.2})^\circ. \quad (\text{A.6})$$

$\mu_1[\text{GeV}]$	2.5	4.2	4.5	4.8	9
$C_1(\mu_1)$	1.13 (1.17)	1.08 (1.12)	1.08 (1.11)	1.07 (1.11)	1.04 (1.07)
$C_2(\mu_1)$	-0.27 (-0.36)	-0.19 (-0.27)	-0.18 (-0.26)	-0.17 (-0.25)	-0.11 (-0.17)
$C_3(\mu_3)$	0.02 (0.02)	0.01 (0.01)	0.01 (0.01)	0.01 (0.01)	0.01 (0.01)
$C_4(\mu_1)$	-0.05 (-0.04)	-0.04 (-0.03)	-0.03 (-0.03)	-0.03 (-0.03)	-0.02 (-0.02)
$C_5(\mu_1)$	0.01 (0.01)	0.01 (0.01)	0.01 (0.01)	0.01 (0.01)	0.01 (0.01)
$C_6(\mu_1)$	-0.06 (-0.05)	-0.04 (-0.03)	-0.04 (-0.03)	-0.04 (-0.03)	-0.03 (-0.02)
$C_8^{\text{eff}}(\mu_1)$	(-0.17)	(-0.15)	(-0.15)	(-0.15)	(-0.14)

Table 5: Values of the Wilson coefficients at NLO(LO)-QCD for different choices of μ_1 .

Regarding the quark masses, we use the kinetic scheme for the b -quark and the $\overline{\text{MS}}$ -scheme for the c -quark:

$$m_b^{\text{kin}}(\mu^{\text{cut}} = 1 \text{ GeV}) = (4.573 \pm 0.012) \text{ GeV} \quad [130], \quad (\text{A.7})$$

$$m_b^{\text{kin}}(\mu^{\text{cut}} = 1 \text{ GeV}) = (4.56 \pm 0.02) \text{ GeV} \quad [131], \quad (\text{A.8})$$

$$\overline{m}_c(\overline{m}_c) = (1.27 \pm 0.02) \text{ GeV} \quad [135]. \quad (\text{A.9})$$

The charm quark mass is then run to the scale $\mu_1 = 4.5 \text{ GeV}$ using the three-loop running implemented in the RunDec package [145]. Concerning the renormalisation scales μ_1 and μ_0 , their central value is set to $\mu_1 = \mu_0 = 4.5 \text{ GeV}$ and we vary both of them independently in the interval $2.25 \text{ GeV} \leq \mu_{1,0} \leq 9 \text{ GeV}$. The running of the Bag parameters \tilde{B}_i^q from $\mu_0 = 1.5 \text{ GeV}$ to $\mu_0 \sim m_b$ is included using the one-loop results given in Refs. [67, 69]. However, we do not include the running of the eye-contractions, as they represent already a NLO effect. The numerical values of the Wilson coefficients, of the decay constants, and of the non-perturbative input needed to parametrise the matrix element of the two- and four-quark operators are summarised respectively in Tables 5, 6 and 7.

Parameter	$B^{+,0}$	Source	B_s^0	Source
f_{B_q} [GeV]	0.1900 ± 0.0013	LQCD [140]	0.2303 ± 0.0013	LQCD [140]
$\bar{\Lambda}_q$ [GeV]	0.5 ± 0.1	Sum Rules [96]	0.6 ± 0.1	Sum Rules [96]
$\mu_\pi^2(B_q)$ [GeV ²]	0.477 ± 0.056	Exp. fit [130]	0.587 ± 0.064	Exp. fit + Eq. (2.49)
	0.43 ± 0.24	Exp. fit [131]	0.47 ± 0.24	Exp. fit + Eq. (2.48)
$\mu_G^2(B_q)$ [GeV ²]	0.294 ± 0.054	Exp. fit [130]	0.353 ± 0.071	Exp. fit + Eq. (2.47)
	0.38 ± 0.07	Exp. fit [131]	0.41 ± 0.08	Exp. fit + Eq. (2.46)
$\rho_D^3(B_q)$ [GeV ³]	0.185 ± 0.031	Exp. fit [130]	0.275 ± 0.066	Exp. fit + Eq. (2.50)
	0.03 ± 0.02	Exp. fit [131]	0.032 ± 0.021	Exp. fit + Eq. (2.51)

Table 6: Numerical values of the non-perturbative parameters used in our analysis. Note that for μ_π^2 , μ_G^2 , and ρ_D^3 , the first line corresponds to Scenario A, and the second one to Scenario B, both defined in Section 2.3.

HQET, $\mu_0 = 1.5$ GeV	\tilde{B}_1	\tilde{B}_2	$\tilde{\epsilon}_1$	$\tilde{\epsilon}_2$
$B^{+,0}$	$1.0026^{+0.0198}_{-0.0106}$	$0.9982^{+0.0052}_{-0.0066}$	$-0.0165^{+0.0209}_{-0.0346}$	$-0.0004^{+0.0200}_{-0.0326}$
B_s^0	$1.0022^{+0.0185}_{-0.0099}$	$0.9983^{+0.0052}_{-0.0067}$	$-0.0104^{+0.0202}_{-0.0330}$	$0.0001^{+0.0199}_{-0.0324}$
HQET, $\mu_0 = 1.5$ GeV	$\tilde{\delta}_1$	$\tilde{\delta}_2$	$\tilde{\delta}_3$	$\tilde{\delta}_4$
$\langle B_q \tilde{O}^q B_q \rangle$	$0.0026^{+0.0142}_{-0.0092}$	$-0.0018^{+0.0047}_{-0.0072}$	$-0.0004^{+0.0015}_{-0.0024}$	$0.0003^{+0.0012}_{-0.0008}$
$\langle B_s \tilde{O}^q B_s \rangle$	$0.0025^{+0.0144}_{-0.0093}$	$-0.0018^{+0.0047}_{-0.0072}$	$-0.0004^{+0.0015}_{-0.0024}$	$0.0003^{+0.0012}_{-0.0008}$
$\langle B_q \tilde{O}^s B_q \rangle$	$0.0023^{+0.0140}_{-0.0091}$	$-0.0017^{+0.0046}_{-0.0070}$	$-0.0004^{+0.0015}_{-0.0023}$	$0.0003^{+0.0012}_{-0.0008}$

Table 7: Numerical values of the Bag parameters and of the eye-contractions used in our analysis and determined in Refs. [69, 96]. Here, due to the isospin symmetry, q denotes both either u or d quark.

B Dimension-seven four-quark operator contribution in VIA

In this section we list the complete expressions for the dimension-seven contribution to the PI, WE and WA diagrams depicted in Fig. 3. For non-leptonic modes, these are symmetric functions of the masses of the two internal quarks and depend on one dimensionless mass parameter $\rho = m_c^2/m_b^2$. We stress that the matrix elements of the dimension-seven HQET

operators have been evaluated in VIA. We, respectively obtain

$$\Gamma_7^{\text{WE}}(\rho, 0) = \Gamma_0 32\pi^2 \left(3C_2^2 + C_1^2 \right) \rho^2 (1 - \rho) \frac{f_{B_q}^2 m_{B_q} \bar{\Lambda}_q}{m_b^4}, \quad (\text{B.1})$$

$$\Gamma_7^{\text{WE}}(\rho, \rho) = \Gamma_0 64\pi^2 \left(3C_2^2 + C_1^2 \right) \frac{\rho^2}{\sqrt{1 - 4\rho}} \frac{f_{B_q}^2 m_{B_q} \bar{\Lambda}_q}{m_b^4}, \quad (\text{B.2})$$

$$\Gamma_7^{\text{PI}}(\rho, 0) = -\Gamma_0 32\pi^2 \left(C_1^2 + 6C_1 C_2 + C_2^2 \right) (1 - \rho)(1 + \rho) \frac{f_{B_q}^2 m_{B_q} \bar{\Lambda}_q}{m_b^4}, \quad (\text{B.3})$$

$$\Gamma_7^{\text{PI}}(\rho, \rho) = -\Gamma_0 32\pi^2 \left(C_1^2 + 6C_1 C_2 + C_2^2 \right) \frac{(1 - 2\rho - 4\rho^2)}{\sqrt{1 - 4\rho}} \frac{f_{B_q}^2 m_{B_q} \bar{\Lambda}_q}{m_b^4}, \quad (\text{B.4})$$

where the corresponding results for the WA topology can be derived from those for WE by exchanging $C_1 \leftrightarrow C_2$. Moreover, in Eqs. (B.1) - (B.4), Γ_0 is defined in Eq. (2.20), while

$$\bar{\Lambda}_q = m_{B_q} - m_b. \quad (\text{B.5})$$

Note, that for internal massless quarks, it is sufficient to take the limit $\rho \rightarrow 0$ in the expressions above, and that due to helicity suppression, both WE and WA results vanish in this case. Finally, for the semileptonic modes, only the WA topology is relevant, and the corresponding expression can be obtained from Eq. (B.1), setting

$$3C_2^2 \rightarrow 1, \quad C_1 \rightarrow 0, \quad \rho \rightarrow \eta = \frac{m_\tau^2}{m_b^2}. \quad (\text{B.6})$$

References

- [1] Y. Amhis et al., *Averages of b-hadron, c-hadron, and τ -lepton properties as of 2021*, [arXiv:2206.07501](https://arxiv.org/abs/2206.07501).
- [2] DELPHI Collaboration, J. Abdallah et al., *A Precise measurement of the B^+ , B^0 and mean b hadron lifetime with the DELPHI detector at LEP1*, *Eur. Phys. J. C* **33** (2004) 307–324, [[hep-ex/0401025](https://arxiv.org/abs/hep-ex/0401025)].
- [3] ALEPH Collaboration, R. Barate et al., *Measurement of the \bar{B}^0 and B^- meson lifetimes*, *Phys. Lett. B* **492** (2000) 275–287, [[hep-ex/0008016](https://arxiv.org/abs/hep-ex/0008016)].
- [4] ALEPH Collaboration, D. Buskulic et al., *Improved measurement of the \bar{B}^0 and B^- meson lifetimes*, *Z. Phys. C* **71** (1996) 31–44.
- [5] DELPHI Collaboration, P. Abreu et al., *A Measurement of B^+ and B^0 lifetimes using $\bar{D}\ell^+$ events*, *Z. Phys. C* **68** (1995) 13–24.
- [6] DELPHI Collaboration, W. Adam et al., *Lifetimes of charged and neutral B hadrons using event topology*, *Z. Phys. C* **68** (1995) 363–374.
- [7] DELPHI Collaboration, P. Abreu et al., *A Precise measurement of the B_q^0 meson lifetime using a new technique*, *Z. Phys. C* **74** (1997) 19–32. [Erratum: *Z.Phys.C* 75, 579 (1997)].

- [8] **L3** Collaboration, M. Acciarri et al., *Upper limit on the lifetime difference of shortlived and longlived B_s^0 mesons*, Phys. Lett. B **438** (1998) 417–429.
- [9] **OPAL** Collaboration, R. Akers et al., *Improved measurements of the B^0 and B^+ meson lifetimes*, Z. Phys. C **67** (1995) 379–388.
- [10] **OPAL** Collaboration, G. Abbiendi et al., *Measurement of the B^+ and B^0 lifetimes and search for $CP(T)$ violation using reconstructed secondary vertices*, Eur. Phys. J. C **12** (2000) 609–626, [[hep-ex/9901017](#)].
- [11] **OPAL** Collaboration, G. Abbiendi et al., *Measurement of the B^0 lifetime and oscillation frequency using $\bar{B}^0 \rightarrow D^{*+}\ell^-$ anti-neutrino decays*, Phys. Lett. B **493** (2000) 266–280, [[hep-ex/0010013](#)].
- [12] **SLD** Collaboration, K. Abe et al., *Measurement of the B^+ and B^0 lifetimes using topological reconstruction of inclusive and semileptonic decays*, Phys. Rev. Lett. **79** (1997) 590–596.
- [13] **CDF** Collaboration, F. Abe et al., *Improved measurement of the B^- and \bar{B}^0 meson lifetimes using semileptonic decays*, Phys. Rev. D **58** (1998) 092002, [[hep-ex/9806018](#)].
- [14] **CDF** Collaboration, D. Acosta et al., *Measurement of B meson lifetimes using fully reconstructed B decays produced in $p\bar{p}$ collisions at $\sqrt{s} = 1.8$ TeV*, Phys. Rev. D **65** (2002) 092009.
- [15] **CDF** Collaboration, T. Aaltonen et al., *Measurement of b Hadron Lifetimes in Exclusive Decays Containing a J/ψ in $p^- pbar$ Collisions at $\sqrt{s} = 1.96$ TeV*, Phys. Rev. Lett. **106** (2011) 121804, [[arXiv:1012.3138](#)].
- [16] **D0** Collaboration, V. M. Abazov et al., *Measurement of the angular and lifetime parameters of the decays $B_d^0 \rightarrow J/\psi K^{*0}$ and $B_s^0 \rightarrow J/\psi \phi$* , Phys. Rev. Lett. **102** (2009) 032001, [[arXiv:0810.0037](#)].
- [17] **D0** Collaboration, V. M. Abazov et al., *Measurement of the Λ_b^0 lifetime in the exclusive decay $\Lambda_b^0 \rightarrow J/\psi \Lambda^0$ in $p\bar{p}$ collisions at $\sqrt{s} = 1.96$ TeV*, Phys. Rev. D **85** (2012) 112003, [[arXiv:1204.2340](#)].
- [18] **D0** Collaboration, V. M. Abazov et al., *Measurement of the B_s^0 Lifetime in the Flavor-Specific Decay Channel $B_s^0 \rightarrow D_s^- \mu^+ \nu X$* , Phys. Rev. Lett. **114** (2015), no. 6 062001, [[arXiv:1410.1568](#)].
- [19] **BaBar** Collaboration, B. Aubert et al., *Measurement of the B^0 and B^+ meson lifetimes with fully reconstructed hadronic final states*, Phys. Rev. Lett. **87** (2001) 201803, [[hep-ex/0107019](#)].
- [20] **BaBar** Collaboration, B. Aubert et al., *Measurement of the B^0 lifetime with partially reconstructed $B^0 \rightarrow D^{*-}\ell + \nu_\ell$ decays*, Phys. Rev. Lett. **89** (2002) 011802, [[hep-ex/0202005](#)]. [Erratum: Phys.Rev.Lett. 89, 169903 (2002)].
- [21] **BaBar** Collaboration, B. Aubert et al., *Simultaneous measurement of the B^0 meson lifetime and mixing frequency with $B^0 \rightarrow D^{*-}\ell^+ \nu_\ell$ decays*, Phys. Rev. D **67** (2003) 072002, [[hep-ex/0212017](#)].

- [22] **BaBar** Collaboration, B. Aubert et al., *Measurement of the B^0 meson lifetime with partial reconstruction of $B^0 \rightarrow D^{*-}\pi^+$ and $B^0 \rightarrow D^{*-}\rho^+$ decays*, Phys. Rev. D **67** (2003) 091101, [[hep-ex/0212012](#)].
- [23] **BaBar** Collaboration, B. Aubert et al., *Measurement of the \bar{B}^0 lifetime and the $B^0\bar{B}^0$ oscillation frequency using partially reconstructed $\bar{B}^0 \rightarrow D^{*+}\ell^-\bar{\nu}_\ell$ decays*, Phys. Rev. D **73** (2006) 012004, [[hep-ex/0507054](#)].
- [24] **Belle** Collaboration, K. Abe et al., *Improved measurement of CP-violation parameters $\sin 2\phi(1)$ and $|\lambda|$, B meson lifetimes, and B^0 - anti- B^0 mixing parameter $\Delta m(d)$* , Phys. Rev. D **71** (2005) 072003, [[hep-ex/0408111](#)]. [Erratum: Phys.Rev.D 71, 079903 (2005)].
- [25] **ATLAS** Collaboration, G. Aad et al., *Measurement of the Λ_b^0 lifetime and mass in the ATLAS experiment*, Phys. Rev. D **87** (2013), no. 3 032002, [[arXiv:1207.2284](#)].
- [26] **CMS** Collaboration, A. M. Sirunyan et al., *Measurement of b hadron lifetimes in pp collisions at $\sqrt{s} = 8$ TeV*, Eur. Phys. J. C **78** (2018), no. 6 457, [[arXiv:1710.08949](#)]. [Erratum: Eur.Phys.J.C 78, 561 (2018)].
- [27] **LHCb** Collaboration, R. Aaij et al., *Measurements of the B^+ , B^0 , B_s^0 meson and Λ_b^0 baryon lifetimes*, JHEP **04** (2014) 114, [[arXiv:1402.2554](#)].
- [28] **LHCb** Collaboration, R. Aaij et al., *Effective lifetime measurements in the $B_s^0 \rightarrow K^+K^-$, $B^0 \rightarrow K^+\pi^-$ and $B_s^0 \rightarrow \pi^+K^-$ decays*, Phys. Lett. B **736** (2014) 446–454, [[arXiv:1406.7204](#)].
- [29] **CDF** Collaboration, T. Aaltonen et al., *Measurement of the B^- Lifetime using a Simulation Free Approach for Trigger Bias Correction*, Phys. Rev. D **83** (2011) 032008, [[arXiv:1004.4855](#)].
- [30] **D0** Collaboration, V. M. Abazov et al., *Measurement of the ratio of B^+ and B^0 meson lifetimes*, Phys. Rev. Lett. **94** (2005) 182001, [[hep-ex/0410052](#)].
- [31] **ALEPH** Collaboration, R. Barate et al., *Study of B_s^0 oscillations and lifetime using fully reconstructed D_s^- decays*, Eur. Phys. J. C **4** (1998) 367–385.
- [32] **DELPHI** Collaboration, P. Abreu et al., *Study of $B^0(S)$ anti- $B^0(S)$ oscillations and $B^0(S)$ lifetimes using hadronic decays of $B^0(S)$ mesons*, Eur. Phys. J. C **18** (2000) 229–252, [[hep-ex/0105077](#)].
- [33] **OPAL** Collaboration, K. Ackerstaff et al., *A Measurement of the B_s^0 lifetime using reconstructed D_s^- mesons*, Eur. Phys. J. C **2** (1998) 407–416, [[hep-ex/9708023](#)].
- [34] **CDF** Collaboration, F. Abe et al., *Measurement of the B_s^0 meson lifetime using semileptonic decays*, Phys. Rev. D **59** (1999) 032004, [[hep-ex/9808003](#)].
- [35] **DELPHI** Collaboration, P. Abreu et al., *Measurement of the B_s^0 lifetime and study of $B_s^0 - \bar{B}_s^0$ oscillations using $D_s\ell$ events*, Eur. Phys. J. C **16** (2000) 555, [[hep-ex/0107077](#)].
- [36] **OPAL** Collaboration, K. Ackerstaff et al., *Measurements of the B_s^0 and Λ_b^0 lifetimes*, Phys. Lett. B **426** (1998) 161–179, [[hep-ex/9802002](#)].

- [37] **CDF** Collaboration, T. Aaltonen et al., *Measurement of the B_s Lifetime in Fully and Partially Reconstructed $B_s \rightarrow D_s^-(\phi\pi^-)X$ Decays in $\bar{p} - p$ Collisions at $\sqrt{s} = 1.96$ TeV*, Phys. Rev. Lett. **107** (2011) 272001, [[arXiv:1103.1864](#)].
- [38] **LHCb** Collaboration, R. Aaij et al., *Measurement of the $\bar{B}_s^0 \rightarrow D_s^- D_s^+$ and $\bar{B}_s^0 \rightarrow D^- D_s^+$ effective lifetimes*, Phys. Rev. Lett. **112** (2014), no. 11 111802, [[arXiv:1312.1217](#)].
- [39] **LHCb** Collaboration, R. Aaij et al., *Measurement of the \bar{B}_s^0 meson lifetime in $D_s^+ \pi^-$ decays*, Phys. Rev. Lett. **113** (2014), no. 17 172001, [[arXiv:1407.5873](#)].
- [40] **LHCb** Collaboration, R. Aaij et al., *Measurement of B_s^0 and D_s^- meson lifetimes*, Phys. Rev. Lett. **119** (2017), no. 10 101801, [[arXiv:1705.03475](#)].
- [41] **CDF** Collaboration, F. Abe et al., *Measurement of B hadron lifetimes using J/ψ final states at CDF*, Phys. Rev. D **57** (1998) 5382–5401.
- [42] **D0** Collaboration, V. M. Abazov et al., *Measurement of the B_s^0 lifetime in the exclusive decay channel $B_s^0 \rightarrow J/\psi\phi$* , Phys. Rev. Lett. **94** (2005) 042001, [[hep-ex/0409043](#)].
- [43] **LHCb** Collaboration, R. Aaij et al., *Measurement of the $B_s^0 \rightarrow \mu^+ \mu^-$ decay properties and search for the $B^0 \rightarrow \mu^+ \mu^-$ and $B_s^0 \rightarrow \mu^+ \mu^- \gamma$ decays*, Phys. Rev. D **105** (2022), no. 1 012010, [[arXiv:2108.09283](#)].
- [44] **CMS** Collaboration, A. M. Sirunyan et al., *Measurement of properties of $B_s^0 \rightarrow \mu^+ \mu^-$ decays and search for $B^0 \rightarrow \mu^+ \mu^-$ with the CMS experiment*, JHEP **04** (2020) 188, [[arXiv:1910.12127](#)].
- [45] **ALEPH** Collaboration, R. Barate et al., *A Study of the decay width difference in the $B_s^0 - \bar{B}_s^0$ system using $\phi\phi$ correlations*, Phys. Lett. B **486** (2000) 286–299.
- [46] **LHCb** Collaboration, R. Aaij et al., *Measurement of the effective $B_s^0 \rightarrow K^+ K^-$ lifetime*, Phys. Lett. B **707** (2012) 349–356, [[arXiv:1111.0521](#)].
- [47] **LHCb** Collaboration, R. Aaij et al., *Measurement of the effective $B_s^0 \rightarrow J/\psi K_S^0$ lifetime*, Nucl. Phys. B **873** (2013) 275–292, [[arXiv:1304.4500](#)].
- [48] **CDF** Collaboration, T. Aaltonen et al., *Measurement of branching ratio and B_s^0 lifetime in the decay $B_s^0 \rightarrow J/\psi f_0(980)$ at CDF*, Phys. Rev. D **84** (2011) 052012, [[arXiv:1106.3682](#)].
- [49] **D0** Collaboration, V. M. Abazov et al., *B_s^0 lifetime measurement in the CP-odd decay channel $B_s^0 \rightarrow J/\psi f_0(980)$* , Phys. Rev. D **94** (2016), no. 1 012001, [[arXiv:1603.01302](#)].
- [50] **LHCb** Collaboration, R. Aaij et al., *Measurement of the $B_s^0 \rightarrow J/\psi\eta$ lifetime*, Phys. Lett. B **762** (2016) 484–492, [[arXiv:1607.06314](#)].
- [51] **LHCb** Collaboration, R. Aaij et al., *Measurement of CP violation and the B_s^0 meson decay width difference with $B_s^0 \rightarrow J/\psi K^+ K^-$ and $B_s^0 \rightarrow J/\psi \pi^+ \pi^-$ decays*, Phys. Rev. D **87** (2013), no. 11 112010, [[arXiv:1304.2600](#)].
- [52] **CDF** Collaboration, T. Aaltonen et al., *Measurement of the Bottom-Strange Meson Mixing Phase in the Full CDF Data Set*, Phys. Rev. Lett. **109** (2012) 171802, [[arXiv:1208.2967](#)].

- [53] **D0** Collaboration, V. M. Abazov et al., *Measurement of the CP-violating phase $\phi_s^{J/\psi\phi}$ using the flavor-tagged decay $B_s^0 \rightarrow J/\psi\phi$ in 8 fb^{-1} of $p\bar{p}$ collisions*, Phys. Rev. D **85** (2012) 032006, [[arXiv:1109.3166](#)].
- [54] **ATLAS** Collaboration, G. Aad et al., *Flavor tagged time-dependent angular analysis of the $B_s \rightarrow J/\psi\phi$ decay and extraction of $\Delta\Gamma_s$ and the weak phase ϕ_s in ATLAS*, Phys. Rev. D **90** (2014), no. 5 052007, [[arXiv:1407.1796](#)].
- [55] **ATLAS** Collaboration, G. Aad et al., *Measurement of the CP-violating phase ϕ_s and the B_s^0 meson decay width difference with $B_s^0 \rightarrow J/\psi\phi$ decays in ATLAS*, JHEP **08** (2016) 147, [[arXiv:1601.03297](#)].
- [56] **ATLAS** Collaboration, G. Aad et al., *Measurement of the CP-violating phase ϕ_s in $B_s^0 \rightarrow J/\psi\phi$ decays in ATLAS at 13 TeV*, Eur. Phys. J. C **81** (2021), no. 4 342, [[arXiv:2001.07115](#)].
- [57] **CMS** Collaboration, V. Khachatryan et al., *Measurement of the CP-violating weak phase ϕ_s and the decay width difference $\Delta\Gamma_s$ using the $B_s^0 \rightarrow J/\psi\phi(1020)$ decay channel in pp collisions at $\sqrt{s} = 8 \text{ TeV}$* , Phys. Lett. B **757** (2016) 97–120, [[arXiv:1507.07527](#)].
- [58] **CMS** Collaboration, A. M. Sirunyan et al., *Measurement of the CP-violating phase ϕ_s in the $B_s^0 \rightarrow J/\psi\phi(1020) \rightarrow \mu^+\mu^-K^+K^-$ channel in proton-proton collisions at $\sqrt{s} = 13 \text{ TeV}$* , Phys. Lett. B **816** (2021) 136188, [[arXiv:2007.02434](#)].
- [59] **LHCb** Collaboration, R. Aaij et al., *Precision measurement of CP violation in $B_s^0 \rightarrow J/\psi K^+K^-$ decays*, Phys. Rev. Lett. **114** (2015), no. 4 041801, [[arXiv:1411.3104](#)].
- [60] **LHCb** Collaboration, R. Aaij et al., *Resonances and CP violation in B_s^0 and $\bar{B}_s^0 \rightarrow J/\psi K^+K^-$ decays in the mass region above the $\phi(1020)$* , JHEP **08** (2017) 037, [[arXiv:1704.08217](#)].
- [61] **LHCb** Collaboration, R. Aaij et al., *First study of the CP-violating phase and decay-width difference in $B_s^0 \rightarrow \psi(2S)\phi$ decays*, Phys. Lett. B **762** (2016) 253–262, [[arXiv:1608.04855](#)].
- [62] **LHCb** Collaboration, R. Aaij et al., *Measurement of the CP-violating phase ϕ_s from $B_s^0 \rightarrow J/\psi\pi^+\pi^-$ decays in 13 TeV pp collisions*, Phys. Lett. B **797** (2019) 134789, [[arXiv:1903.05530](#)].
- [63] **LHCb** Collaboration, R. Aaij et al., *Updated measurement of time-dependent CP-violating observables in $B_s^0 \rightarrow J/\psi K^+K^-$ decays*, Eur. Phys. J. C **79** (2019), no. 8 706, [[arXiv:1906.08356](#)]. [Erratum: Eur.Phys.J.C 80, 601 (2020)].
- [64] **LHCb** Collaboration, R. Aaij et al., *First measurement of the CP-violating phase in $B_s^0 \rightarrow J/\psi(\rightarrow e^+e^-)\phi$ decays*, Eur. Phys. J. C **81** (2021), no. 11 1026, [[arXiv:2105.14738](#)].
- [65] A. Lenz, *Lifetimes and heavy quark expansion*, Int. J. Mod. Phys. A **30** (2015), no. 10 1543005, [[arXiv:1405.3601](#)].
- [66] M. A. Shifman and M. B. Voloshin, *Hierarchy of Lifetimes of Charmed and Beautiful Hadrons*, Sov. Phys. JETP **64** (1986) 698. [Zh. Eksp. Teor. Fiz.91,1180(1986)].
- [67] M. Neubert and C. T. Sachrajda, *Spectator effects in inclusive decays of beauty hadrons*, Nucl. Phys. B **483** (1997) 339–370, [[hep-ph/9603202](#)].

- [68] F. Gabbiani, A. I. Onishchenko, and A. A. Petrov, *Spectator effects and lifetimes of heavy hadrons*, Phys. Rev. **D70** (2004) 094031, [[hep-ph/0407004](#)].
- [69] M. Kirk, A. Lenz, and T. Rauh, *Dimension-six matrix elements for meson mixing and lifetimes from sum rules*, JHEP **12** (2017) 068, [[arXiv:1711.02100](#)]. [Erratum: JHEP **06**, 162 (2020)].
- [70] M. Beneke and G. Buchalla, *The B_c Meson Lifetime*, Phys. Rev. D **53** (1996) 4991–5000, [[hep-ph/9601249](#)].
- [71] J. Aebischer and B. Grinstein, *Standard Model prediction of the B_c lifetime*, JHEP **07** (2021) 130, [[arXiv:2105.02988](#)].
- [72] J. Aebischer and B. Grinstein, *A novel determination of the B_c lifetime*, [[arXiv:2108.10285](#)].
- [73] D. King, A. Lenz, M. L. Piscopo, T. Rauh, A. V. Rusov, and C. Vlahos, *Revisiting Inclusive Decay Widths of Charmed Mesons*, [[arXiv:2109.13219](#)].
- [74] J. Gratx, B. Melić, and I. Nišandžić, *Lifetimes of singly charmed hadrons*, JHEP **07** (2022) 058, [[arXiv:2204.11935](#)].
- [75] C. Bobeth, U. Haisch, A. Lenz, B. Pecjak, and G. Tetlalmatzi-Xolocotzi, *On new physics in $\Delta\Gamma_d$* , JHEP **06** (2014) 040, [[arXiv:1404.2531](#)].
- [76] J. Brod, A. Lenz, G. Tetlalmatzi-Xolocotzi, and M. Wiebusch, *New physics effects in tree-level decays and the precision in the determination of the quark mixing angle γ* , Phys. Rev. D **92** (2015), no. 3 033002, [[arXiv:1412.1446](#)].
- [77] S. Jäger, M. Kirk, A. Lenz, and K. Leslie, *Charming new physics in rare B -decays and mixing?*, Phys. Rev. D **97** (2018), no. 1 015021, [[arXiv:1701.09183](#)].
- [78] S. Jäger, M. Kirk, A. Lenz, and K. Leslie, *Charming New B -Physics*, JHEP **03** (2020) 122, [[arXiv:1910.12924](#)].
- [79] A. Lenz and G. Tetlalmatzi-Xolocotzi, *Model-independent bounds on new physics effects in non-leptonic tree-level decays of B -mesons*, JHEP **07** (2020) 177, [[arXiv:1912.07621](#)].
- [80] M. Bordone, N. Gubernari, T. Huber, M. Jung, and D. van Dyk, *A puzzle in $\bar{B}_{(s)}^0 \rightarrow D_{(s)}^{(*)+} \{\pi^-, K^-\}$ decays and extraction of the f_s/f_d fragmentation fraction*, Eur. Phys. J. C **80** (2020), no. 10 951, [[arXiv:2007.10338](#)].
- [81] S. Iguro and T. Kitahara, *Implications for new physics from a novel puzzle in $\bar{B}_{(s)}^0 \rightarrow D_{(s)}^{(*)+} \{\pi^-, K^-\}$ decays*, Phys. Rev. D **102** (2020), no. 7 071701, [[arXiv:2008.01086](#)].
- [82] F.-M. Cai, W.-J. Deng, X.-Q. Li, and Y.-D. Yang, *Probing new physics in class-I B -meson decays into heavy-light final states*, JHEP **10** (2021) 235, [[arXiv:2103.04138](#)].
- [83] C. Bobeth and U. Haisch, *New Physics in Γ_{12}^s : $(\bar{s}b)(\bar{\tau}\tau)$ Operators*, Acta Phys. Polon. **B44** (2013) 127–176, [[arXiv:1109.1826](#)].
- [84] J. F. Kamenik, S. Monteil, A. Semkiv, and L. V. Silva, *Lepton polarization asymmetries in rare semi-tauonic $b \rightarrow s$ exclusive decays at FCC-ee*, Eur. Phys. J. C **77** (2017), no. 10 701, [[arXiv:1705.11106](#)].

- [85] B. Capdevila, A. Crivellin, S. Descotes-Genon, L. Hofer, and J. Matias, *Searching for New Physics with $b \rightarrow s\tau^+\tau^-$ processes*, Phys. Rev. Lett. **120** (2018), no. 18 181802, [[arXiv:1712.01919](#)].
- [86] C. Cornella, G. Isidori, M. König, S. Liechti, P. Owen, and N. Serra, *Hunting for $B^+ \rightarrow K^+\tau^+\tau^-$ imprints on the $B^+ \rightarrow K^+\mu^+\mu^-$ dimuon spectrum*, Eur. Phys. J. C **80** (2020), no. 12 1095, [[arXiv:2001.04470](#)].
- [87] **LHCb** Collaboration, R. Aaij et al., *Search for the decays $B_s^0 \rightarrow \tau^+\tau^-$ and $B^0 \rightarrow \tau^+\tau^-$* , Phys. Rev. Lett. **118** (2017), no. 25 251802, [[arXiv:1703.02508](#)].
- [88] C. Bobeth, M. Gorbahn, T. Hermann, M. Misiak, E. Stamou, and M. Steinhauser, *$B_{s,d} \rightarrow l^+l^-$ in the Standard Model with Reduced Theoretical Uncertainty*, Phys. Rev. Lett. **112** (2014) 101801, [[arXiv:1311.0903](#)].
- [89] G. Elor, M. Escudero, and A. Nelson, *Baryogenesis and Dark Matter from B Mesons*, Phys. Rev. D **99** (2019), no. 3 035031, [[arXiv:1810.00880](#)].
- [90] G. Alonso-Álvarez, G. Elor, and M. Escudero, *Collider signals of baryogenesis and dark matter from B mesons: A roadmap to discovery*, Phys. Rev. D **104** (2021), no. 3 035028, [[arXiv:2101.02706](#)].
- [91] T. Jubb, M. Kirk, A. Lenz, and G. Tetlalmatzi-Xolocotzi, *On the ultimate precision of meson mixing observables*, Nucl. Phys. **B915** (2017) 431–453, [[arXiv:1603.07770](#)].
- [92] A. Lenz, M. L. Piscopo, and A. V. Rusov, *Contribution of the Darwin operator to non-leptonic decays of heavy quarks*, JHEP **12** (2020) 199, [[arXiv:2004.09527](#)].
- [93] T. Mannel, D. Moreno, and A. Pivovarov, *Heavy quark expansion for heavy hadron lifetimes: completing the $1/m_b^3$ corrections*, JHEP **08** (2020) 089, [[arXiv:2004.09485](#)].
- [94] D. Moreno, *Completing $1/m_b^3$ corrections to non-leptonic bottom-to-up-quark decays*, JHEP **01** (2021) 051, [[arXiv:2009.08756](#)].
- [95] M. L. Piscopo, *Higher order corrections to the lifetime of heavy hadrons*. PhD thesis, Siegen U., 2021. [[arXiv:2112.03137](#)].
- [96] D. King, A. Lenz, and T. Rauh, *$SU(3)$ breaking effects in B and D meson lifetimes*, JHEP **06** (2022) 134, [[arXiv:2112.03691](#)].
- [97] D. Becirevic, *Theoretical progress in describing the B meson lifetimes*, PoS HEP2001 (2001) 098, [[hep-ph/0110124](#)].
- [98] G. Buchalla, A. J. Buras, and M. E. Lautenbacher, *Weak decays beyond leading logarithms*, Rev. Mod. Phys. **68** (1996) 1125–1144, [[hep-ph/9512380](#)].
- [99] M. Neubert, *Heavy quark symmetry*, Phys. Rept. **245** (1994) 259–396, [[hep-ph/9306320](#)].
- [100] M. Fael, K. Schönwald, and M. Steinhauser, *Third order corrections to the semileptonic $b \rightarrow c$ and the muon decays*, Phys. Rev. D **104** (2021), no. 1 016003, [[arXiv:2011.13654](#)].
- [101] M. Czakon, A. Czarnecki, and M. Dowling, *Three-loop corrections to the muon and heavy quark decay rates*, Phys. Rev. D **103** (2021) L111301, [[arXiv:2104.05804](#)].

- [102] A. Lenz, U. Nierste, and G. Ostermaier, *Penguin diagrams, charmless B decays and the missing charm puzzle*, Phys. Rev. **D56** (1997) 7228–7239, [[hep-ph/9706501](#)].
- [103] A. Lenz, U. Nierste, and G. Ostermaier, *Determination of the CKM angle γ and $|V_{ub}/V_{cb}|$ from inclusive direct CP asymmetries and branching ratios in charmless B decays*, Phys. Rev. **D59** (1999) 034008, [[hep-ph/9802202](#)].
- [104] Q. Ho-kim and X.-Y. Pham, *Exact One Gluon Corrections for Inclusive Weak Processes*, Annals Phys. **155** (1984) 202.
- [105] F. Krinner, A. Lenz, and T. Rauh, *The inclusive decay $b \rightarrow c\bar{c}s$ revisited*, Nucl. Phys. **B876** (2013) 31–54, [[arXiv:1305.5390](#)].
- [106] E. Bagan, P. Ball, V. M. Braun, and P. Gosdzinsky, *Charm quark mass dependence of QCD corrections to nonleptonic inclusive B decays*, Nucl. Phys. **B432** (1994) 3–38, [[hep-ph/9408306](#)].
- [107] T. Mannel, A. A. Pivovarov, and D. Rosenthal, *Inclusive weak decays of heavy hadrons with power suppressed terms at NLO*, Phys. Rev. **D92** (2015), no. 5 054025, [[arXiv:1506.08167](#)].
- [108] B. Blok and M. A. Shifman, *The Rule of discarding $1/N_c$ in inclusive weak decays. 2.*, Nucl. Phys. **B399** (1993) 459–476, [[hep-ph/9209289](#)].
- [109] B. Blok and M. A. Shifman, *The Rule of discarding $1/N_c$ in inclusive weak decays. 1.*, Nucl. Phys. **B399** (1993) 441–458, [[hep-ph/9207236](#)].
- [110] I. I. Y. Bigi, B. Blok, M. A. Shifman, N. G. Uraltsev, and A. I. Vainshtein, *A QCD ‘manifesto’ on inclusive decays of beauty and charm*, in The Fermilab Meeting DPF 92. Proceedings, 7th Meeting of the American Physical Society, Division of Pa pp. 610–613, 1992. [[hep-ph/9212227](#)].
- [111] T. Mannel, A. V. Rusov, and F. Shahriaran, *Inclusive semitauonic B decays to order $\mathcal{O}(\Lambda_{QCD}^3/m_b^3)$* , Nucl. Phys. **B921** (2017) 211–224, [[arXiv:1702.01089](#)].
- [112] S. Balk, J. G. Korner, D. Pirjol, and K. Schilcher, *Inclusive semileptonic B decays in QCD including lepton mass effects*, Z. Phys. C **64** (1994) 37–44, [[hep-ph/9312220](#)].
- [113] A. F. Falk, Z. Ligeti, M. Neubert, and Y. Nir, *Heavy quark expansion for the inclusive decay $\bar{B} \rightarrow \tau \bar{\nu}_\tau X$* , Phys. Lett. B **326** (1994) 145–153, [[hep-ph/9401226](#)].
- [114] M. Gremm and A. Kapustin, *Order $1/m_b^3$ corrections to $B \rightarrow X(c)$ lepton anti-neutrino decay and their implication for the measurement of $\bar{\Lambda}$ and λ_1* , Phys. Rev. **D55** (1997) 6924–6932, [[hep-ph/9603448](#)].
- [115] T. Mannel and A. A. Pivovarov, *QCD corrections to inclusive heavy hadron weak decays at Λ_{QCD}^3/m_Q^3* , Phys. Rev. **D100** (2019), no. 9 093001, [[arXiv:1907.09187](#)].
- [116] T. Mannel, D. Moreno, and A. A. Pivovarov, *NLO QCD corrections to inclusive $b \rightarrow c\bar{l}\bar{\nu}$ decay spectra up to $1/m_Q^3$* , Phys. Rev. D **105** (2022), no. 5 054033, [[arXiv:2112.03875](#)].
- [117] D. Moreno, *NLO QCD corrections to inclusive semitauonic weak decays of heavy hadrons up to $1/m_b^3$* , [[arXiv:2207.14245](#)].

- [118] M. Rahimi and K. K. Vos, *Standard Model predictions for Lepton Flavour Universality ratios of inclusive semileptonic B decays*, [arXiv:2207.03432](#).
- [119] N. G. Uraltsev, *On the problem of boosting nonleptonic b baryon decays*, Phys. Lett. **B376** (1996) 303–308, [[hep-ph/9602324](#)].
- [120] E. Franco, V. Lubicz, F. Mescia, and C. Tarantino, *Lifetime ratios of beauty hadrons at the next-to-leading order in QCD*, Nucl. Phys. **B633** (2002) 212–236, [[hep-ph/0203089](#)].
- [121] M. Beneke, G. Buchalla, C. Greub, A. Lenz, and U. Nierste, *The $B^+ - B_d^0$ Lifetime Difference Beyond Leading Logarithms*, Nucl. Phys. **B639** (2002) 389–407, [[hep-ph/0202106](#)].
- [122] A. Lenz and T. Rauh, *D-meson lifetimes within the heavy quark expansion*, Phys. Rev. **D88** (2013) 034004, [[arXiv:1305.3588](#)].
- [123] F. Gabbiani, A. I. Onishchenko, and A. A. Petrov, Λ_b lifetime puzzle in heavy quark expansion, Phys. Rev. D **68** (2003) 114006, [[hep-ph/0303235](#)].
- [124] M. Neubert, *Heavy meson form-factors from QCD sum rules*, Phys. Rev. D **45** (1992) 2451–2466.
- [125] M. Neubert, *Symmetry breaking corrections to meson decay constants in the heavy quark effective theory*, Phys. Rev. D **46** (1992) 1076–1087.
- [126] W. Kilian and T. Mannel, *QCD corrected $1/m_b$ contributions to $B - \bar{B}$ mixing*, Phys. Lett. B **301** (1993) 382–392, [[hep-ph/9211333](#)].
- [127] B. M. Dassinger, T. Mannel, and S. Turczyk, *Inclusive semi-leptonic B decays to order $1/m_b^4$* , JHEP **03** (2007) 087, [[hep-ph/0611168](#)].
- [128] A. Alberti, P. Gambino, K. J. Healey, and S. Nandi, *Precision Determination of the Cabibbo-Kobayashi-Maskawa Element V_{cb}* , Phys. Rev. Lett. **114** (2015), no. 6 061802, [[arXiv:1411.6560](#)].
- [129] P. Gambino, K. J. Healey, and S. Turczyk, *Taming the higher power corrections in semileptonic B decays*, Phys. Lett. B **763** (2016) 60–65, [[arXiv:1606.06174](#)].
- [130] M. Bordone, B. Capdevila, and P. Gambino, *Three loop calculations and inclusive V_{cb}* , Phys. Lett. B **822** (2021) 136679, [[arXiv:2107.00604](#)].
- [131] F. Bernlochner, M. Fael, K. Olschewsky, E. Persson, R. van Tonder, K. K. Vos, and M. Welsch, *First extraction of inclusive V_{cb} from q^2 moments*, [arXiv:2205.10274](#).
- [132] Belle Collaboration, R. van Tonder et al., *Measurements of q^2 Moments of Inclusive $B \rightarrow X_c \ell^+ \nu_\ell$ Decays with Hadronic Tagging*, Phys. Rev. D **104** (2021), no. 11 112011, [[arXiv:2109.01685](#)].
- [133] Belle-II Collaboration, *Measurement of Lepton Mass Squared Moments in $B \rightarrow X_c \ell \bar{\nu}_\ell$ Decays with the Belle II Experiment*, [arXiv:2205.06372](#).
- [134] N. Uraltsev, *On the chromomagnetic expectation value μ_G^2 and higher power corrections in heavy flavor mesons*, Phys. Lett. B **545** (2002) 337–344, [[hep-ph/0111166](#)].
- [135] Particle Data Group Collaboration, P. Zyla et al., *Review of Particle Physics*, PTEP **2020** (2020), no. 8 083C01.

- [136] P. Gambino, A. Melis, and S. Simula, *Extraction of heavy-quark-expansion parameters from unquenched lattice data on pseudoscalar and vector heavy-light meson masses*, Phys. Rev. D **96** (2017), no. 1 014511, [[arXiv:1704.06105](#)].
- [137] P. Gambino, V. Lubicz, A. Melis, and S. Simula, *Masses, decay constants and HQE matrix elements of pseudoscalar and vector heavy-light mesons in LQCD*, J. Phys. Conf. Ser. **1137** (2019), no. 1 012005.
- [138] M. Bordone and P. Gambino, *The semileptonic B_s and Λ_b widths*, in 11th International Workshop on the CKM Unitarity Triangle, 3, 2022. [arXiv:2203.13107](#).
- [139] I. I. Bigi, T. Mannel, and N. Uraltsev, *Semileptonic width ratios among beauty hadrons*, JHEP **09** (2011) 012, [[arXiv:1105.4574](#)].
- [140] **Flavour Lattice Averaging Group** Collaboration, S. Aoki et al., *FLAG Review 2019: Flavour Lattice Averaging Group (FLAG)*, Eur. Phys. J. C **80** (2020), no. 2 113, [[arXiv:1902.08191](#)].
- [141] I. I. Y. Bigi, M. A. Shifman, N. G. Uraltsev, and A. I. Vainshtein, *Sum rules for heavy flavor transitions in the SV limit*, Phys. Rev. D **52** (1995) 196–235, [[hep-ph/9405410](#)].
- [142] I. I. Y. Bigi, M. A. Shifman, N. Uraltsev, and A. I. Vainshtein, *High power n of m_b in beauty widths and $n = 5 \rightarrow \infty$ limit*, Phys. Rev. D **56** (1997) 4017–4030, [[hep-ph/9704245](#)].
- [143] W. A. Bardeen, A. J. Buras, D. W. Duke, and T. Muta, *Deep Inelastic Scattering Beyond the Leading Order in Asymptotically Free Gauge Theories*, Phys. Rev. D **18** (1978) 3998.
- [144] A. Czarnecki, M. Slusarczyk, and F. V. Tkachov, *Enhancement of the hadronic b quark decays*, Phys. Rev. Lett. **96** (2006) 171803, [[hep-ph/0511004](#)].
- [145] F. Herren and M. Steinhauser, *Version 3 of RunDec and CRunDec*, Comput. Phys. Commun. **224** (2018) 333–345, [[arXiv:1703.03751](#)].
- [146] **CKMfitter Group** Collaboration, J. Charles, A. Hocker, H. Lacker, S. Laplace, F. R. Le Diberder, J. Malcles, J. Ocariz, M. Pivk, and L. Roos, *CP violation and the CKM matrix: Assessing the impact of the asymmetric B factories*, Eur. Phys. J. C **41** (2005), no. 1 1–131, [[hep-ph/0406184](#)].